INVESTIGATION OF REAL TIME DNA REPAIR VIA SURFACE PLASMON RESONANCE (SPR)

by

Enis Demir

A Thesis Submitted to the

Graduate School of Sciences and Engineering

in Partial Fulfillment of the Requirements for

the Degree of

Master of Science

in

Chemical and Biological Engineering

Koç University

August, 2011

Koç University

Graduate School of Sciences and Engineering

This is to certify that I have examined this copy of a master's thesis by

Enis Demir

and have found that it is complete and satisfactory in all respects,

and that any and all revisions required by the final

examining committee have been made.

Committee Members:

_____

Seda Kızılel Ph.D. (Advisor)

_____

Halil Kavaklı Ph.D.

_____

Gülayşe İnce Dunn Ph.D.

Date: _____

ACKNOWLEDGEMENT

This work has been carried out in the the period of August 2009-August 2010 at the Department of Chemical Engineering, Koç University under the guidance of **Assist. Prof. Seda Kızılel**.

To begin with, I would like to express my appreciation and gratitude to my supervisor, Assist. Prof. Seda Kızılel for giving me the opportunity to accomplish my M. Sc. Study under her guidance. I also would like to thank her for accepting me as her M. Sc. student, introducing me to the subject, and guiding me through the research. I am extremely grateful to **Assoc. Prof. Halil Kavaklı** for his assistance on all of my research projects, and valuable advice and discussions. I am also grateful to Assist. Prof. Gulayse Ince Dunn for critical reading and useful comments in this thesis.

I am also especially thankful to **Dr. Rıza Kızılel** for his guidance throughout this project and invaluable help on all parts of my study.

I would like to thank **Selimcan Azizoğlu** (Department of Chemical Engineering) for his great help to this project and his assistance in SPR assays.

I would like to thank also **Hande Asimgil, Ph.D.** (Department of Materials Sciences and Engineering) for her assistance in my research.

I would like to thank my friends, **Bilal Çakır, Onur Dağlıyan, Erdal Uzunlar, Sibel Kalyoncu, Onur Öztaş, Selmi Bozbağ, Seda Giray, Ezgi Dağyıldız, Nil Ezgi Dinçer, İbrahim Gür**, **Işıl Tulum,** who have been both my office-mates and valuable colleagues for the period of M.Sc. education and study. I also thank to the Graduate School of Engineering of Koç University for their help in all student affairs.

And last but not least, I would like to thank especially **my family** and **Zeynep Ülker** for their endless and unconditional support, and love during my life and education.

ABSTRACT

DNA structure can be greatly affected by UV light exposure. The cyclobutane prymidine dimer (CPD) and 6-4 lesion formations along with the specific breaks on strands are the most common type of DNA damage caused by UV irradiation. Specific to UV-damaged DNA, CPD photolyase I and II construct two subfamilies of flavoproteins, and they have recognition and repair capabilities of CPD sites on both single stranded (ssDNA) and double stranded (dsDNA) DNA with the aid of blue light energy. The other types of flavoprotein family consist of cryptochromes (CRY), and the most commonly known types act as photoreceptors in plants, or circadian rhythm regulators in animals, but lack photorepair activity. Recently, it has been found that a specific type of cryptochrome also has photorepair activity on ssDNA. This protein, called cryptochrome-DASH (CRY-DASH), is yet to be studied for its binding to DNA with newly developed techniques. In this thesis, CRY-DASH-DNA interaction was investigated using Surface Plasmon Resonance (SPR) which is a common assay to characterize protein-DNA or protein-protein interactions. Next, interaction of UV damaged and undamaged DNA with CPD photolyase was then examined and compared with the interaction of damaged/undamaged DNA and CRY-DASH. SPR shows the immediate molecular binding of DNA to the surface and confirms the specific binding of photolyase and CRY-DASH with UV treated or UV untreated DNA by providing kinetic constants of binding. This study is significant for investigation of repair of lesions in the DNA structure using SPR.

ÖZET

UV ışığına maruz kalan canlıların DNA yapısında büyük değişimler görülebilir. Siklobütan primidin dimerlerin (CPD) ve 6-4 lezyonlarının oluşumu bu değişimlerin en sık gözlemlenenleridir. Bir flavoprotein alt ailesine ait olan CPD I ve II fotoliaz enzimleri DNA üzerinde UV ışığı ile hasar görmüş bu bölgelere spesifik bağlanarak, hasarlı bölgelerin tamirini üstlenir. Mavi ışık enerjisini kullanarak tek zincrili ve çift zincirli DNA'ların UV-hasarlı bölgelerini tamir eden bu protein ailesine akraba olan kriptokromlar ise DNA tamirinden çok, bitkilerde ışık reseptörü, memelilerde ise sirkadiyan saatin önemli bir bileşeni olarak metabolizma içinde görev alır. Bu bilgiye rağmen, oldukça yeni keşfedilen bir kriptokrom çeşidinin de UV ışığı ile hasarlanmış tek zincirli DNA'yı fotoliaz enzimi gibi tamir edebildiği gözlemlenmiştir. CRY-DASH adı verilen bu protein henüz yeterli miktarda araştırmaya konu olmamıştır. Bu tezde, tek zincirli ve çift zincirli DNA'nın CRY-DASH ile etkileşimi, tamir süreci Yüzey Plazmon Rezonansı (SPR) adı verilen bir teknik yardımı ile incelenmiş olup, bu etkileşimin DNA-fotoliaz enzimi etkileşimi ile karılaştırması yapılarak CRY-DASH'in DNA'ya bağlanma etkinliği ölçülmüştür.SPR sayesinde CRY-DASH'in ve fotoliaz'ın DNA anlık bağlanması, bu bağlanmanın spesifikliği kinetik parametrelerin de hesaplanması ile görülmüştür. Bu çalışma DNA üzerindeki lezyonların tamirini SPR yöntemi ile göstermesi açısından önemlidir.

to my family…

TABLE OF CONTENTS

LIST OF TABLES

LIST OF FIGURES

Chapter 1

1. INTRODUCTION

Flavins are ubiquitous redox-active catalysts in one- and two-electron transfer reactions, and flavoproteins are involved in a wide variety of redox transformations in bioenergetics, including photosynthesis and respiration [1]. In this thesis, a specific subclass of the DNA photolyase/cryptochrome family proteins of CRY-DASH is studied in order to investigate DNA repair via SPR. Although proteins from this family share a great portion of sequence, 3D formation, and redox-active flavin adenine dinucleotide (FAD) cofactor, their function differs in a broad range of activities such as capability of DNA repair via blue light energy, being main components of the circadian clock and plant growth metabolism. The most basic difference between the functions of photolyases and cryptochromes is considered to be caused by the presence of C-terminal or N-terminal extensions in cryptochromes, which are responsible in mediating the signal transduction step [2].

CRY-DASH is a relatively new member of the DNA photolyase/cryptochrome family. Although recent data indicates that the DASH cryptochromes are single-strand-specific cyclobutane prymidine dimer (CPD)-photolyases, there are relatively few studies focused on this function of the protein, which requires additional confirmation. To investigate the interaction between single-stranded DNA and CRY-DASH, Surface Plasmon Resonance (SPR) spectroscopy is employed in this study.

In this thesis, Chapter 2 introduces our protein of interest, CRY-DASH, and briefly gives background information about cryptochrome/photolyase protein family while the emphasis is on CRY-DASH.

In Chapter 3, the theoretical background on SPR spectroscopy is provided, including basic principles of SPR, SPR sensor surface chemistry, general applications, and principles of kinetic and equilibrium analysis in SPR.

The materials and procedures for DNA sample preparation, and experimental setup used for SPR instruments are given in three separate sections in Chapter 5.

In Chapter 6, the kinetic data collected by SPR is reported. The efficiency of the experimental procedure is also dicussed in this chapter. And finally, the general conclusion and future directions about this study are provided in Chapter 7.

Chapter 2

2. DNA Damage and Repair

Light is the absolute necessity for life on earth. Nearly all living organisms on earth benefit from sun light as an energy source. The ultraviolet (UV) range of sun light first contributed to the birth of life as the main energy source to produce organic molecules. Secondly, its ability also to damage DNA is especially important as a major reason for further evolution of the organisms [3].

The Earth had not have the ozone layer to absorb most of harmful UV light, before the first forms of life began to produce oxygen. It was not possible at that moment to survive without an appropriate protection mechanism against UV irradiation. For that purpose, living organisms acquired evolutionary repair abilities to prevent DNA damage caused by UV or other types of factors. One of the repair mechanisms that organisms gained and developed is “the photorepairing”. The enzyme family responsible for the photorepair is called *DNA photolyases*. They form more diverse protein family together with their evolutionarily relatives, *Cryptochromes*- the DNA *photolyase/cryptochrome* family. *Cryptochromes* are different than *Photolyases* in terms of function in the cell, in which they control hypocotyl growth and the transition to flowering in plants and are the main components of the circadian clock in animals [3, 4].

In the current work, the emphasis is going to be on the DASH type of protein of Cryptochrome family, which actually behaves like a DNA photolyase while repairing single stranded DNA as much as its former relative protein [5].

2.1 DNA Repair

The sources of damage to DNA vary between the endogeneous – caused by metabolic by-products or replication errors- or exogeneous –external factors such as some toxins and UV light. The endogeneous damage is usually caused by self dynamics of the metabolism of the cell, whereas the exogeneous damage factors have a wide range of examples including: mutagenic chemicals, chemotherapy and radiotherapy, some viruses, X-rays and UV irradiation, which can produce bulky adducts on DNA bases, or even break DNA phosphate-sugar backbone [6, 7]. DNA repair is the process of restoring DNA after damage. It consists of a multi-enzyme, multi-pathway system that keeps the genetic material in the cell intact and viable [8].

2.2 Photoproducts

UV light consists of three spectral regions that can cause mutagenic, or even lethal effects on living organisms: UV-A (320-400 nm), UV-B (280-320 nm), and UV-C (100-280 nm). The effect of radiation at wavelengths approaching absorption maximum of DNA (at around 260 nm) is converting a pyrimidine base to an excited state. The excited base can react with other molecules to form unstable intermediates or stable photoproducts which results in cyclobutane pyrimidine dimer (CPD) and pyrimidine (6-4) photoproducts ((6-4)PPs) due to the covalent link formation between adjacent pyrimidines within the same DNA strand. The irradiated DNA forms includes 70 - 80 % CPDs and 20-30% (6-4)PPs (Figure 1). These four base-ring photoproducts can be lethal to cell metabolism because of the blockage of the DNA/RNA polymerases on the same DNA strand or halting polymerase progression during both DNA replication or transcription[9-11]. The most possible reason behind skin cancer are the formation of these photoproducts [8, 12]. It is thought to be caused by generation of mutations in tumor suppressor genes, such as p53, which are expresses in UV-induced skin tumors[13, 14].

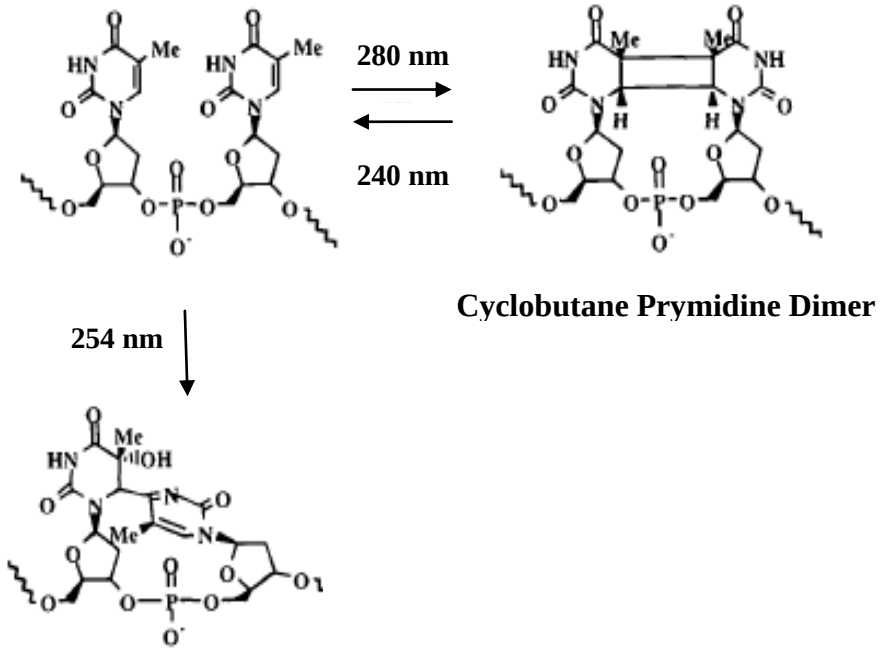

Figure 2.1 Formation of T-T byproducts through UV irradiation

2.3 DNA Repair Proteins

The DNA photolyase/ cryptochrome family is divided into several subclasses according to sequence similarity and function (Figure 2.1). DNA photolyases are enzymes that repair the DNA lesions induced by CPDs and (6-4) photoproducts by using light energy in the UV-A region[15].

Flavin adenine dinucleotide (FAD) is the catalytic cofactor of DNA photolyase when it is in its fully reduced form ($FADH^-$). Catalysis happens through electron transfer from the excited catalytic cofactor to the UV-B photoproduct, splitting the cyclobutane or oxetane rings, and backtransfer electron to the semireduced FADH° [16].

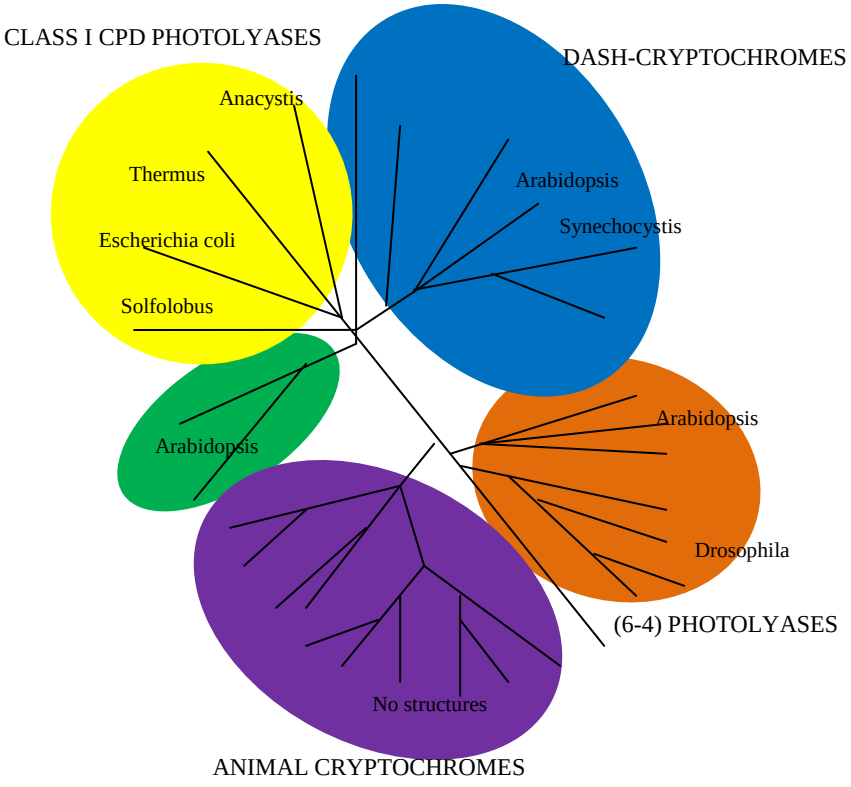

Figure 2.2 Phylogenetic tree of representative members of the cryptochrome/ photolyase family, adapted from [17].

One way of excitation of FAD is through direct photon absorption. Despite cryptochromes and DNA photolyases share considerable sequence and structural composition, cryptochromes(cry) specialize in photoreceptor function, and photolyase

(PHR) specialize in repair. In plants, crptochromes are mainly responsible in hypocotyl growth and transition to flowering whereas they act as a main component of circadian clock in mammalians [18, 19].

The more recently discovered subclass of the cryptochrome/photolyse family, called CRY DASH, is found in cyanobacteria, eubacteria, and vertebrates [20, 21]. They lacked repair activity for CPDs in double-stranded DNA (dsDNA), so they were suggested as photoreceptors –controlling the circadian clock- despite their DNA-binding activity in single-stranded DNA(ssDNA)[18, 19]. The crystal structure of CRY-DASH is determined for *Synechocystis* CRY-DASH [22] and *Arabidopsis thaliana (A. t.*) cry3 [23], and the overall protein folds are found to be similar to class I CPD photolyases [24, 25]. The structural similarity is mostly based on an N-terminal α/β-domain and a C-terminal α-domain with the FAD cofactor inside a U-shaped conformation. Similar to photolyases, FAD is fully reduced to $FADH^-$ form(catalytically active form) during photoactivation[23, 26]. The surface features around the FAD-binding pocket of cry3 and *Synechocystis* CRY-DASH have been found to be essential for DNA binding as in DNA photolyase[27]. Despite the similarity, it has to be mentioned that CRY-DASH proteins lack the C-terminal extensions which are present in plant and animal cryptochromes and thought to give them the signaling activity. However, it was shown that DASH cryptochromes repair CPDs specifically in single-stranded DNA (ssDNA)[5], and therefore there has been emerging necessity of classification of DASH type cryptochromes as ssDNA-specific photolyases. It was hypothesized that the ssDNA repair activity is a relict of an evolutionary period when lateral gene transfer in the form of ssDNA viruses and free ssDNA played an important role.

In this study, photolyase/cryptochrome genes of the *Vibrio cholerae* were particularly used. The three genes found in *V. cholerae* belong to this family according to the sequences

of VcEl Tor VcN16961. These three photolyase may be allowing *V. cholerae* to photorepair the CPDs and the (6-4) photoproducts [28].

Chapter 3

3. SPR

3.1 Theoretical Background on SPR

During 1990s, the invention of the commercial SPR biosensor opened the way to quantitatively and qualitatively characterize the reversible interactions between molecules disregarding any contaminating methods involving labeling of the molecules. SPR biosensors measure the change in the refractive index to detect the specific, reversible binding of an analyte to an immobilized binding partner. This technique allows measuring the kinetic constants and binding affinities of macromolecular interactions.

Several studies ongoing and using SPR include receptor-ligand interactions[29, 30], antibody-antigen interactions [31-33], virus research [34, 35] and etc.

3.2 Principles of SPR

Long before the physical phenomenon of surface plasmon resonance has advanced to the extent where it has been used for practical applications in sensitive detectors [36], it was first observed by Wood, in which he saw that the polarized light gave several light and dark bands when projected on a mirror with a grated surface. A complete understanding and some minimal use could be achieved in 1968 by Otto, and its use in biomolecular interactions was done in 1983 by Liedberg. In mid 1980s, SPR was started to be used in immunochemical assays. Today's simple liquid handling system comes from the principle that light cannot pass to a lower refractive index medium, which is liquid, when it comes from a higher refractive index medium, which is a prism, and is therefore reflected at the thin metal layer on sensor surface (Figure 3).

3.2.1 Basic Principle of SPR

A more basic explanation for working principle of SPR which is otherwise quite complex, covers the knowledge that an SPR instrument measures the refractive index change near a sensor surface (within ~300 nm) using an optical method. The sensor surface forms a flow cell with a solution running over continuously. It also contains the molecule (the ligand) that is to be immobilized on. The other molecule of interest, which is the binding partner, the analyte, is injected with the running solution over the flow cell. The binding of the analyte to its ligand and its accumulation on the surface increases the refractive index. The change in refractive index is recorded real-time by the instrument and, and the recorded data is plotted in response units (RU) versus time, whereas the RU means approximately 1 pg protein/mm^2 [37].

3.2.2 SPR Instrument

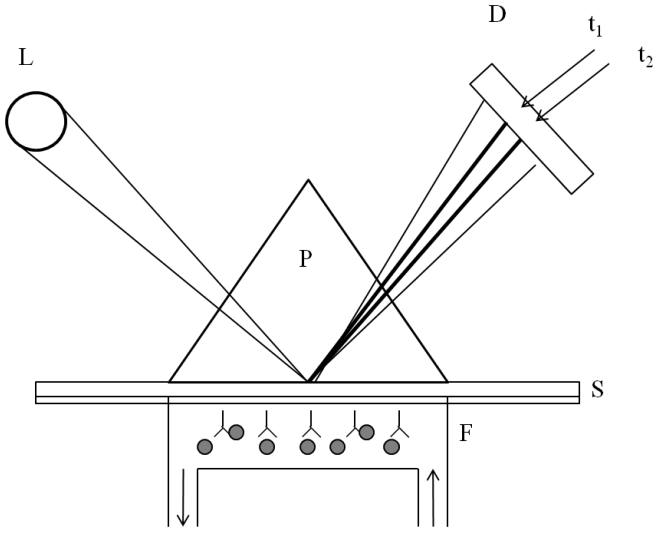

Figure 3.1 A basic SPR instrumental setup. L: Light source, P: Glass prism, D: Photodiode array, S: Sample surface, F: Flow, t1: Data collected at time t1, t2: Data collected at time t2.

There are various specificities among instruments from different manufacturers; however most of the protocols outlined should be adaptable in most cases. The detection unit of a standard SPR instrument is shown in the Figure 3.1. A monochromatic, plane-polarized light source is optically connected with a photo-detector through a glass prism (P). The glass prism contains a thin metal film positioned on (S), which is itself in contact with the sample solution. The incident light beam is on the back side of the metal film is totally reflected on to the diode-array detector. And at the time the wave function of the light incident on the metal film couples to oscillations of the conducting electrons – called plasmons - at the metal surface, surface plasmon resonance occurs. The electromagnetic field created by these oscillations is referred as the evanescent wave. This wave extends from the metal surface into the sample solution. At a precisely determined angle, the plasmon resonance decreases the intensity of the reflected light sharply. This new angle - called the SPR angle – depends on the refractive index change close to the metal surface. The shifts in SPR angle depend only on refractive index changes of a thin layer adjacent to the metal surface. The wavelength of the light source and the metal of the film are also important instrumental parameters. If the SPR angle shift is monitored over time, a gradual increase of material at the surface will cause a successive increase of the SPR angle, which is detected as a shift of the position of the light intensity minimum on the diode array. The SPR angle shifts obtained from different proteins in solution have been correlated to surface concentration determined from radio-labeling techniques and found to be linear within a wide range of surface concentration. The instrument output, the resonance signal, is given in resonance units (RU); 1,000 RU corresponds to a 0.1° shift in the SPR angle, and for an average protein this is equivalent to a surface concentration change of about 1ng/mm^2. It should be noted that, the relationship between RU change and surface concentration may be different for non-protein species. It has been reported that for DNA

780 RU = 0.1° shift [38, 39], but this has been disputed recently with a claim that nucleic acids and protein have similar dependencies [40].

3.2.3 SPR Methods for Reversible Interactions

Several studies on macromolecular interactions using SPR imaging has been published last decade. Most of these studies have been done in the field of T-cell antigen-receptor and major histo-compatibility complex (MHC)-encoded molecules [41, 42], antibody-antigen interactions [32, 33], protein-carbohydrate interactions [43], DNA-DNA and protein-DNA interactions [38, 44]. A typical biosensor experiment involves attaching one reactant to the sensor surface at first. Then, a second reactant is introduced at constant concentration into the buffer flow above, so that the association of the reactants takes place, and this complex formation on the sensor surface is monitored. The dissociation phase occurs subsequently when the buffer flow is passed with zero concentration of the free mobile reactant. As a final step, the sensor surface is regenerated to remove the remaining complex. The association, dissociation and regeneration processes are cycled for different concentrations of the mobile reactant. The principle of SPR is demonstrated in figure 4 which shows the interaction of DNA with a compound in solution buffer.

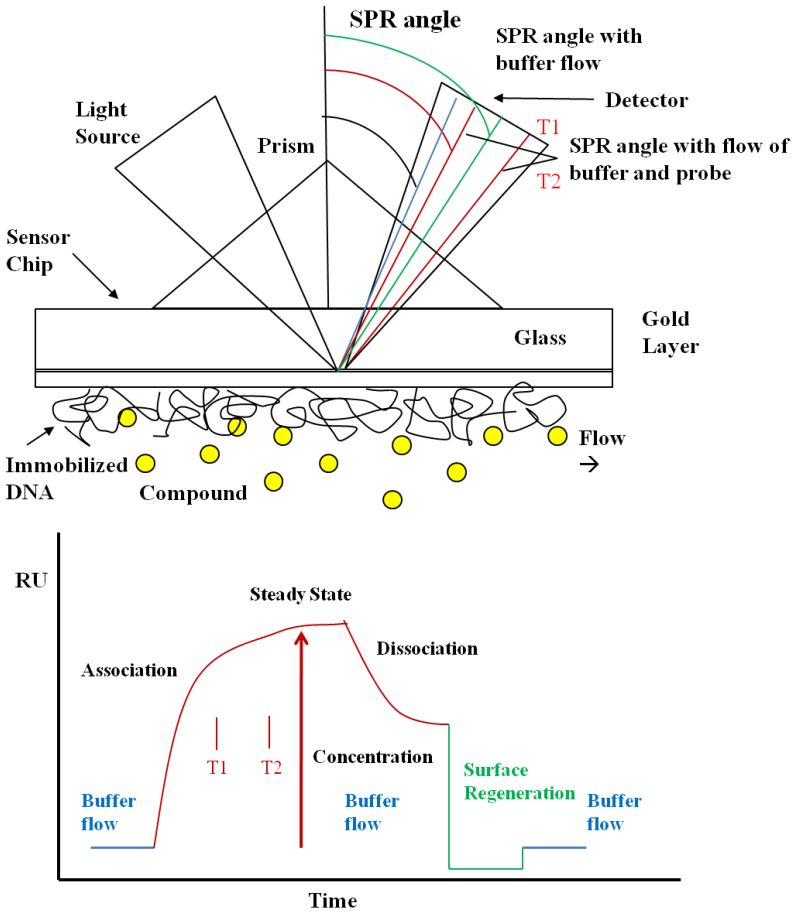

Figure 3.2 Representation of SPR principle

For quantitative characterization of chemical binding kinetics and equilibrium, the use of evanescent wave biosensors requires some techniques to be followed in order to successfully monitor pseudo-fist-order kinetics. The general rules to be satisfied are as follows:

1. The immobile reactant must attach to the surface in native conformation, and most importantly in a uniformly accessible and reactive orientation. The sensor surface must also be prepared to reduce non-specific binding to insignificant amounts.
2. Most biological macromolecules create small refractive index increments which require high concentration of binding sites at the sensor surface (possibly between 10-100 μM range).
3. The efficient transport of the mobile reactant to the sensor surface is important to successfully measure the binding progress which is generally limited by the mass transport issues and the steric hindrance caused by neighboring binding sites at the sensor surface. The binding processes are also affected by the rebinding of the mobile reactants to other binding sites available during both association and dissociation phases. A typical biosensor experiment mostly includes the minimization of these problems and for development of more advanced experimental techniques.

Despite the difficulties needed to overcome, the versatility of the SPR technique allows it to be used as a tool for the analysis of equilibrium and kinetic rate constants of reversible interactions of biomolecules.

3.2.4 Sensor Surface and Immobilization

The first step of the SPR technique requires one of the binding partners to be immobilized on the sensor surface. It is important to keep the non-specific binding at minimum so that the measure binding mainly reflects the native interaction of the binding partners. The requirement of uniform orientation of the immobilized reactant and unrestrained accessibility of the mobile reactant is fulfilled to successfully attach the macromolecule. Therefore the sensor surface and immobilization technique is very important and even the best choice of which binding partner to immobilize and which

immobilization technique is used depends on the particular set of the interacting macromolecules.

The gold surface of the sensor chip used in this study is covered with oligoethylene oxides in order to prevent non-specific binding and to create a hydrophilic surface. This flexible, negatively charged molecule allows for preventing non-specific electrostatic adsorption which may interfere with the requirements for a kinetic analysis along with high immobilization densities. In this case, it is advantageous to use a planar sensor surface. The specific 2D planar chemistry of Sensiq Biosensors (Nomadics, Inc.) prevents possible artifacts. This also creates a biocompatible environment where the immobilized reactant remains soluble.

In most of the biosensor applications, sensor surfaces are attached with carboxymethylated dextran matrix which can be further modified to allow for a variety of immobilization chemistries [45, 46]. The Sensiq Biosensors include planar carboxyl (COOH) chemistries for kinetic optimization methods; biotin and avidin modified gold surfaces for small reagent capture, histidine-capture surfaces for polyhistidine-tag ligand capture etc. The biotin and avidin modified sensor surfaces uses the method of indirect coupling while exploiting the high affinity of biotin-avidin interaction [47, 48]. This method is preferred for DNA or RNA immobilization onto the sensor surface [48, 49].

3.3 Applications of SPR

3.3.1 Evaluation of Macromolecules

For recombinant protein technology, it is important to be able to show that the recombinant protein has the same structure as its native counterpart. With the possible exception of enzymes, confirmation of a protein binding with its natural ligand proves the structural similarity between the recombinant and the native protein. Because such

interactions involve multiple residues, which are usually far apart in the primary amino acid sequence, they require a correctly folded protein. In the absence of natural ligands monoclonal antibodies (mAbs) that are known to bind to the native protein are excellent means of assessing the structural integrity of the recombinant protein. The SPR instrument is particularly well suited to the evaluation of binding of recombinant proteins to natural ligands and mAbs. It is relatively fast to set up an assay for a particular protein and provide highly informative data.

3.3.2 Equilibrium Measurements

Equilibrium analysis requires a very time consuming, multiple sequential injections of analyte at different concentrations (and at different temperatures). The dissociation rate constant or k_d determines the time it takes to reach equilibrium.

$$K_D = {}^{k_d}/_{k_a} \tag{3.1}$$

Whereas K_D is the equilibrium dissociation constant, and k_a is the association constant.

It is considered that an interaction should reach 99% of the equilibrium level within $4.6/k_d$ seconds. Due to the very slow k_d values, high affinity interactions, with a K_D smaller than 10 nM, are usually unsuitable for equilibrium analysis. Conversely, very weak interactions (K_D >100 μM) can be characterized relatively easily.

3.3.3 Kinetic Measurements

The capability of real-time binding measurement makes SPR well suited to the analysis of binding kinetics. Kinetic analysis consists of some shortcomings that are usually caused by mass transport limitations which again makes it difficult to measure accurately k_a values faster than about 10^6 M^{-1} s^{-1} (dependent on the size of the analyte).

Faster k_a values can be measured with analytes with a greater molecular mass. This is because the larger signal produced by a large analyte allows for the experiment to be performed at lower ligand densities, and lower ligand densities require lower rates of mass transport. For different reasons measuring k_d values slower than 10^{-5} s^{-1} or faster than ~1 s^{-1} is difficult. It should be noted that obtaining accurate kinetic data is a very demanding task, which also requires a thorough understanding of binding kinetics and the potential sources of artifact.

3.4 Data Analysis

3.4.1 Biomolecular Interaction Model

The biomolecular interaction between the ligand (L) and the mobile reactant analyte (A) can be modeled in the form of a 1:1 complex AL, with the chemical association rate constant k_a, the dissociation rate constant k_d and the thermochemical equilibrium dissociation constant K_D (Equation 3.1).

$$L + A \underset{k_d}{\overset{k_a}{\rightleftharpoons}} L + A$$

After assuming a constant concentration of the mobile reactant in the buffer flow and infinitely fast exchange with bulk solution, we can write the pseudo-first-order rate equation as follows:

$$\frac{d[AL]}{dt} = k_a[L]([A]_{tot} - [AL]) - k_d[AL] \quad (3.2)$$

whereas $[A]_{tot}$: total binding capacity of the surface

With the biosensor response R proportional to [AL], equation 3.2 gives:

$$\frac{dR}{dt} = k_a f_0 R_{sat} - (k_a f_0 + k_d) R \quad (3.3)$$

where f_0 represents [L], and R_{sat} represents the response at complete saturation of the immobilized binding sites, $[A]_{tot}$.

If the reaction starts with no mobile reactant bound initially, the time function of binding response is described as:

$$R(t) = R_{eq}(f_0)[1 - \exp(-k_{obs} t)] \quad (3.4)$$

where k_{obs} represents observed rate constant expressed as:

$$k_{obs} = k_a f_0 + k_d \quad (3.5)$$

The response signal in equilibrium is given by R_{eq} as follows:

$$R_{eq}(f_0) = R_{max}[1 + \frac{k_d}{k_d f_0}]^{-1} = R_{max}[1 + \frac{K_D}{f_0}]^{-1} \quad (3.6)$$

During dissociation phase the free mobile reactant is removed from the buffer, and for time greater than initial time R(t) is expressed as follows:

$f_0 = 0$ for $t > t_0$; $\quad R(t) = R(t_0) \exp[-k_d (t - t_0)]$ (3.7)

3.4.2 Equilibrium Constants

The analysis of the dependence of the equilibrium plateau signals on the concentration of the analyte (Equation 3.6) determines the thermodynamic equilibrium constant. The equilibrium constant can also be determined from Equation 3.1 as suggested before[50].

$K_D = k_d / k_a$ (3.1)

The binding model excludes the concerns caused by mass transport limitations and therefore may not be significant for the thermodynamic approach of the equilibrium analysis. This model can be preferred for the reactions that are very fast for kinetic analysis [51], however, it is usually not possible to achieve reliable results for very slow reactions, for which it takes too much time to reach equilibrium [52, 53]. As a result, accurate determination of equilibrium constant suffers from baseline drift caused by temperature differences, refractive index mismatches due to the buffer changes, or non-specific binding. In order to tackle with this situation, the results should be compared with those performed in additional reference cells where the response signal is monitored in the absence of immobilized reactant[54].

3.4.3 Analysis of Binding Kinetics

Equations (3.4) and (3.7) given in the previous section determine the equilibrium signal for 1:1 interaction as proposed by pseudo-first-order kinetics.

Two different data analysis strategies have been proposed to extract the rate constants k_{obs} and k_d: linear regression of plots of dR/dt versus R for the association phase and $\ln[R(t_0)/R(t)]$ versus time for the dissociation phase; alternatively, a nonlinear fit with the integrated rate equations (Equations 3.4–3.7) may be used [53]. Although equivalent in principle, except for the more advantageous error distributions in the nonlinear regression, these strategies differ in their potential for ease of extension to account for the influence of mass transport.

3.4.4 Mass Transport Limitations

The most common problem with the kinetic biosensor experiments is that the binding kinetics becomes often limited by the transport rate of the mobile reactant from bulk flow to the sensor surface. An insufficient rate of transport prevents the user to obtain

meaningful kinetic information. The fast rate of biological macromolecules are predicted around 10^6 $M^{-1}sec^{-1}$ [55].

In concept, mass transport limitation can be described as the failure to maintain the bulk concentration, f_0, of the free mobile reactant at the sensor surface at the border of the binding sites [55]. In description, the competition between the immobilized binding sites for a limited supply of binding partner and a local depletion of mobile reactant characterizes the association phase of a fast surface-binding reaction near the surface. In this case, the mass transport rate limits the association, and the measured binding-progress curve can deviate from an exponential shape as described in equation (3.4) [55]. For the case of the dissociation phase, if the transport rate is exceeded by the rate of dissociation, the accumulating concentration of mobile reactant in the vicinity of the sensor surface allows for rebinding to empty binding sites [56, 57]. This can cause a significant deviation from a single exponential dissociation process due to a slower overall dissociation from the surface [58].

The approximate compartment model used most commonly in case of significant mass transport limitation is given as follows [59, 60]:

$$\frac{k_a^{app}}{k_a} = \frac{k_d^{app}}{k_d} = [1 + k_a(R_{sat} - R)k_{tr}]^{-1} \quad (3.8)$$

where k_a^{app} and k_d^{app} are apparent rate constants of association and dissociation phases and k_{tr} is the phenomenological transport rate constant. Equation (3.8) accounts for the binding capacity of the sensor and the effects of mass transport on both association and dissociation phases although it gives a very simplified understanding of the mass transport limitation in the process. More accurate information can be achieved through computational models used by data analysis programs such as Qdat program used for Sensiq SPR instruments (Nomadics, Inc.). In the results section, more detailed global fitting model used by the analysis program will be provided.

Although binding models taking the mass transport limitations into account provide more accurate data about binding kinetics, the most useful solutions to transport issues are experimental precautions used to lower the effect of mass transport on binding kinetics. First, it is recommended to use the lowest possible binding capacity, a higher buffer flow rate and to add a binding competitor to the dissociation buffer. The experimental setup to minimize the effect of mass transport limitation is detailed in the discussion section.

Chapter 4

4. Materials and Methods

4.1 Sample Preparation

As introduced in Chapter 2, the repair proteins analyzed and discussed in this work are the following: wild type *V. Chlorae* photolyase *(*VcPHR), wild type *V. Chlorae* class I cryptochrome (VcCRYI).

4.1.1 Proteins of the DNA Photolyase/Cryptochrome Family

VcPHR was prepared as described previously[61] and supplied from Prof. Halil Kavakli's laboratory (Department of Chemical and Biological Engineering, Koc University).

The plasmids encoding pUNC2001 (MBP-VcPhr), pUNC2002 (MBP-VcCry1) [61] were amplified by PCR using primers based on the genomic sequence provided by Hsu et al[28]. *V. cholerae* 01 El Tor genomic DNA and the amplified genes were inserted into pMal-c2, and The cloned genes were completely sequenced to ensure that no mutation was introduced during PCR amplification VcCRY I was overproduced in *E. coli*, purified. All protein samples were stored at -20 ^{0}C after purification.

4.1.2 UV Irradiation

The substrate DNA was irradiated at a fluence of 50 J/m^2 UV light at 254nm, and at a fluence rate of 0.5 J/m^{2}s (Slyvania G8W). This requires a period of 1 minute to achieve the target extent of UV irradiation, which corresponds to 50 J/m^2. The UV fluencies were measured using a UVX digital radiometer (Ultraviolet Products Inc.) with the appropriate sensor detecting UV light at 254nm. CPD formation was showed with the decrease in

absorbance (10 mm path length) at wavelength 260 nm for DNA samples (Figure 4.1). All measurements were done in triplicate in NanoDrop 1000 (Thermo Scientific). The SPR protocol for DNA and the proteins, VcPHR and VcCry I samples were handled separately, and can be followed in the respective sections of SPR methods.

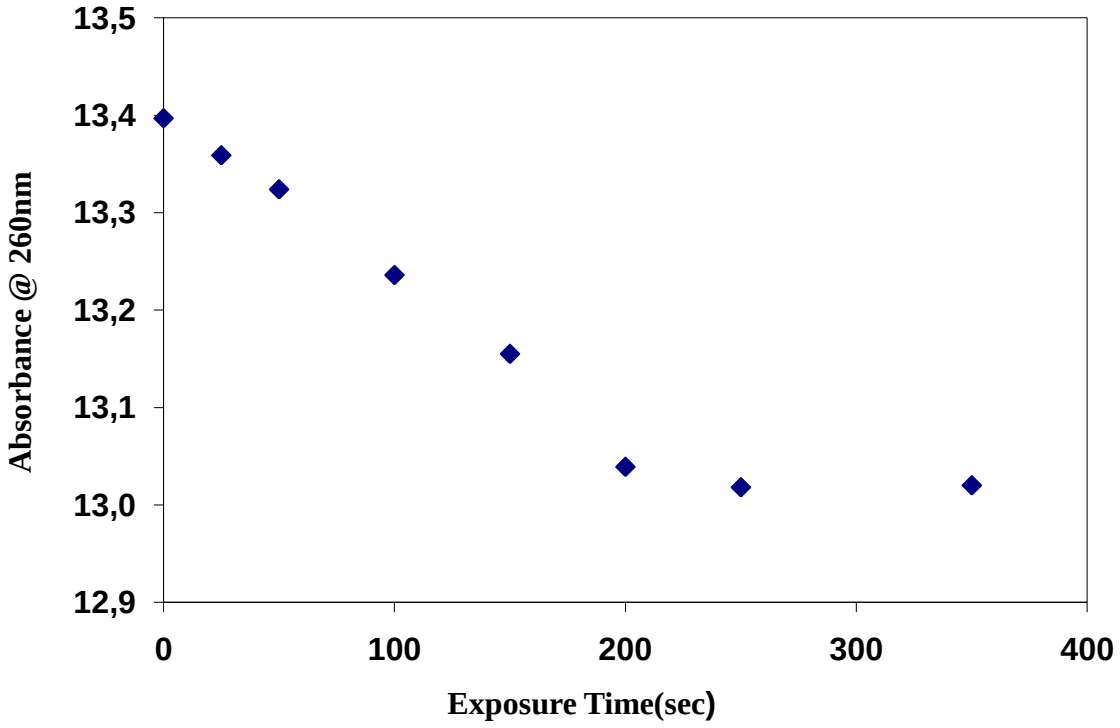

Figure 4.1 Variation in absorbance of the DNA strands that were exposed to UV-irradiation

4.2 SPR Spectroscopy

4.2.1 Reagents and proteins

Immobilization buffer no.1 was prepared from (100 mM PBS, pH 7.0, pH 7.4, 150 mM NaCl), and immobilization buffer no.2 was prepared from one PBS tablet (Sigma Ald.) in 200 mL dH_2O (10 mM phosphate buffer, 2.7 mM KCl, 137 mM NaCl, pH 7.4), 0.005 % Tween20 was aldo used in the running buffers as surfactant to prevent the non-specific protein binding to sensor surface. 100 mM NaOH and 0.1 % SDS are used as regeneration and instrument cleaning solutions due to the significant non-specific protein and DNA binding on the sensor surface. All other reagents were purchased from Sigma Aldrich.

4.2.2 Equipment

First, SPR analysis was performed on a Sensiq Discovery(ICX Nomadics, Oklahama City, OK, USA) system using avidin modified sensor chips (BioCap chip, SensiQ Disc.). Buffer solutions were egassed using a vacuum pump. Buffer pH values were checked with a pH-meter (PHM 210, MeterLab) equipped with a combined pH glass electrode.

4.2.3 Software

All SPR results were acquired using the instrument-bundled software *Sensiq Discovery* (version B.00, build 2.0.0). Data processing and steady state analysis were performed in Qdat Data Analysis Tool (version 1.0.0.24; Nomadics Inc.) which was also used for kinetic analysis (Figure 4.2).

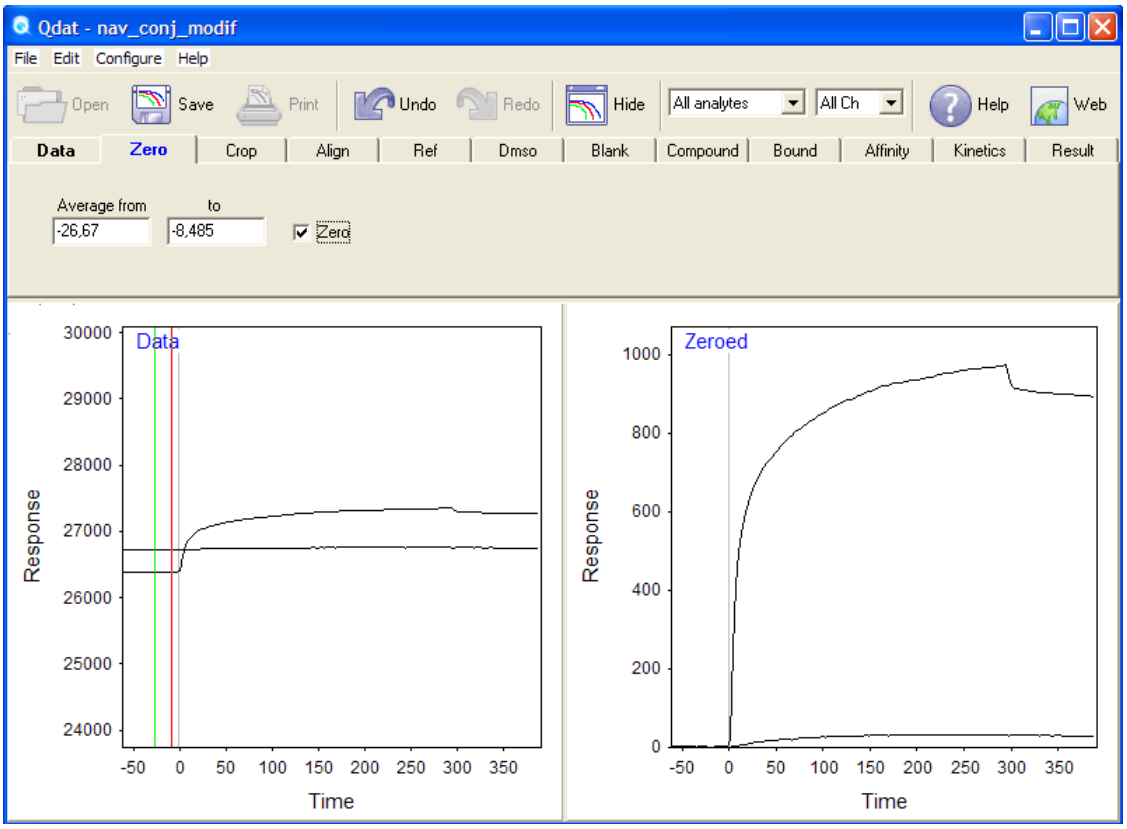

Figure 4.2 The SPR data that is analyzed by Qdat program that processes using Clamp and Scrubber architecture from Biologic Software, Inc.

4.2.4 Preparation of running buffers

All buffers used for Sensiq experiments were filtered to reduce particle load and avoid clogging of the filter frits that are positioned at the entrance of the injection ports. In addition, buffers were degassed every day by keeping them in an ultrasonic bath for at least 15 minutes or keeping them under reduced pressure (< 50 mbar) with the help of a vacuum pump. The basic procedures for preparing samples and buffers was as follows:

All buffers with volume larger than 100 mL were filtered through 0.45 µm filters and degassed at room temperature. Degassing was achieved by filtering under vacuum. All

samples between 3 mL-100 mL was filtered and degassed with the help of the ultrasonicator. The samples with volume less than 3 mL was centrifuged at high spees (5000 Hz) for 5-10 min, and then degassed in a vacuum chamber. Before samples were used, they were centrifuged very briefly to dislodge air-bubbles.All the vials were kept closed to prevent evaporation. The pH of the immobilization buffer was chosen to sufficiently reach a negative charge for the DNA to be immobilized at the surface. The physiologically balanced pH range for DNA and our protein CRY-DASH was between 7.0 and 8.0 as proposed [5] . This was done by injecting constant concentrations of the target protein at pH values at or below its isoelectric point (pI) to a non-activated flow cell and selecting the highest pH, which showed sufficiently high attraction signals.Typically, surface was washed with short pulses of the regeneration solution (NaOH) in order to remove protein, which was bound via electrostatic interaction. The regeneration step also consists of removing non-specific protein binding due to the hydrophobic interactions – with sodium dodecyl sulphate (SDS).

4.2.5 Instrument maintenance

To ensure maximum instrument lifetime but also high data quality, maintenance procedure should be precisely applied as was recommoended by the manufacturer. A correlation between maintenance and data quality was demonstrated in Cannon *et al.* [62]. Cleanin*g* routines (cleaning of the instrument injection ports and buffering lines with 0.1% SDS followed by 100 mM NaOH, pH 13) were performed at least once a week but also between experiment series, as regeneration buffer and in the case of decreased data quality. In addition, the system was rarely turned off but kept under constant flow conditions when an assay was ongoing. After the assays were finished, the system was always cleaned by 0.1 % SDS and then distiled water (dH_2O). The injection port was always blown up with excess dH_2O followed by air. This procedure is repeated 5 times to ensure no buffer

ingredient is present in injection lines. Manual cleaning of the needle, syringes, and the injection port were done on a regular daily basis.

4.2.6 Initial preparation of new sensor chips

In order to remove minor impurities from the chip surface, each sensor chip was treated with the regeneration solutions prior to use (preconditioning). For this purpose, a new sensor chip Biocap (used for immobilization of ssDNA) was inserted and the SPR dip signals (Figure 4.3) were controlled to prevent insufficient normalization for refractive index change during air-buffer transition A dip signal of SPR is caused by a sudden loss of binding signal due to an air bubble, passing over the chip, of which the refractive index (RI) is much lower than RI of the buffer used. The huge refractive index difference creates a sharp drop in response signal . The system then was primed three times with standard PBS buffer (pH 7.4). The response over time data (collected via Sensiq Discovery program) were followed for at least 60 min until a stable baseline for the response was achieved.

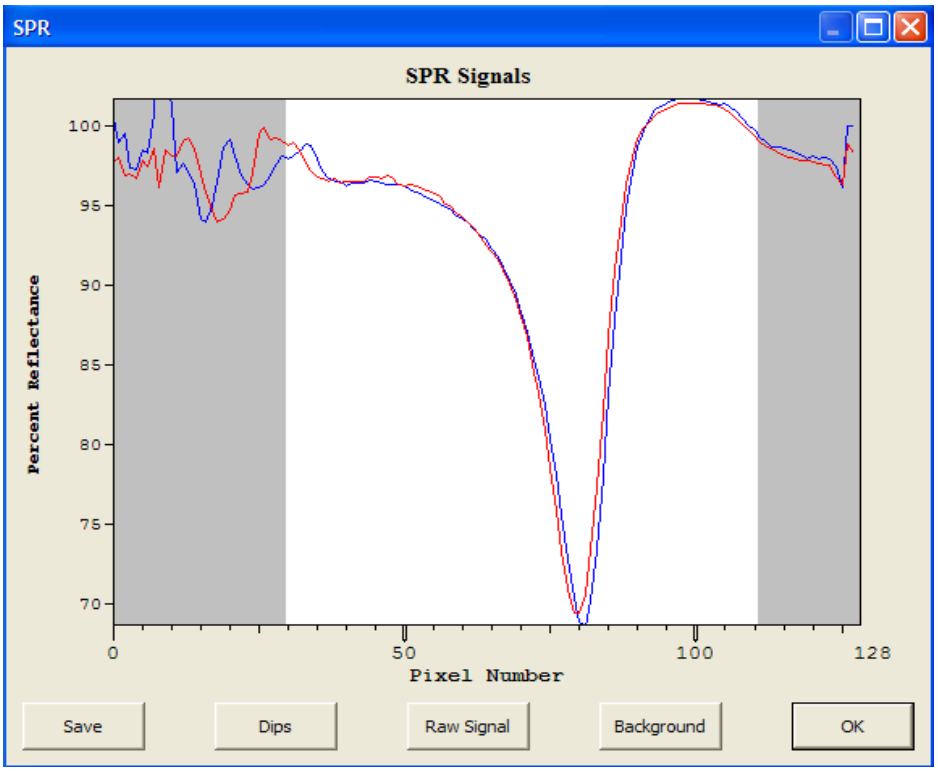

Figure 4.3 The dip signal of the SPR sensor chip used. Red represents the signal in Channel 1, and blue represents the signal in Channel 2.

4.2.7 Data processing

Biosensor result files were directly loaded into *Scrubber* for further processing. After the baseline of all flow cells were overlaid just before injection start, sensorgrams were cropped and injection start points were aligned by Qdat program. The sensorgram of an empty flow cell was subtracted from all the other sensorgrams (reference channel). In order to reduce systematic errors in curve shape, the average of an ensemble of blank injections was subtracted.

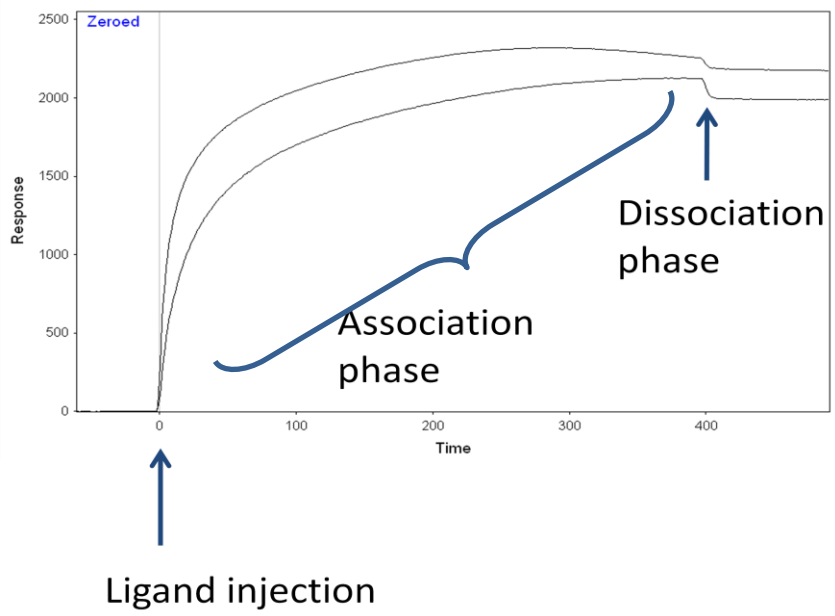

Figure 4.4 Typical SPR response over time graph that SPR data collector program provides

Chapter 5

5. RESULTS

5.1 SPR Results

In this section, the SPR data collected in response over time graphs for both ligand (ssDNA) and analyte (CRY-DASH protein) are demonstrated. For this purpose, the procedure for kinetic analysis in Qdat program was followed and presented as results.

5.1.1 The modification of the sensor surface with Biotin-NHS

Before the ligand Biotin-ssDNA was immobilized; the modification of the BioCap sensor with Biotin-NHS was monitored and investigated briefly to verify the sensor surface activity towards biotin end of the DNA samples (Figure 5.1).

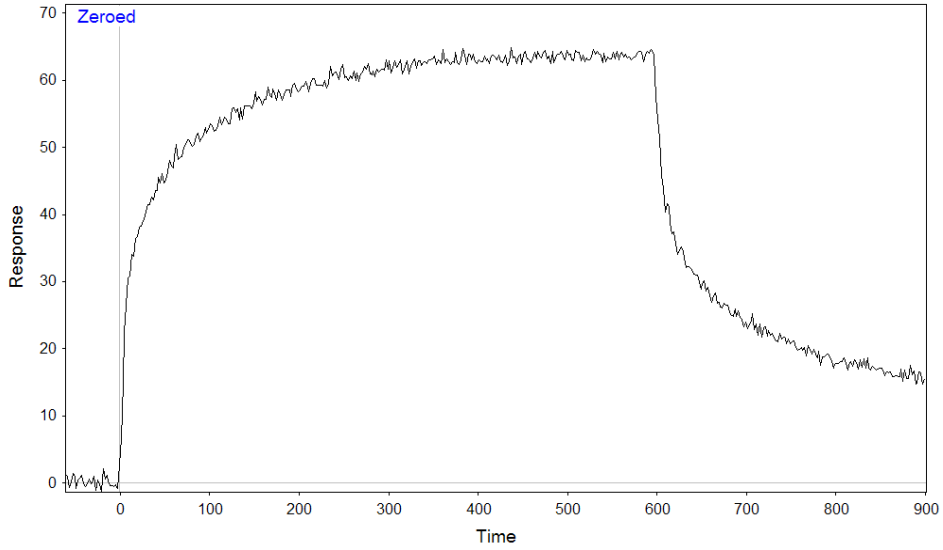

Figure 5.1 The response over time graph for Biotin-NHS pass over BioCap chip.

5.1.2 Ligand Immobilization

The immobilization of biotinylated ssDNA on the sensor surface with a flow rate of 1 mL/min was injected at DNA concentration of 100 nM to achieve adequate number of DNA strands bound on the surface (Figure 5.2). The difference between the response after dissociation phase and the response before association shows the amount of the conjugate immobilized tightly on the sensor surface. UV-irradiated ssDNA was passed through channel 1 (Ch 1), and un-irradiated ssDNA was passed through channel 2 (Ch 2). They are both strongly bound to the surface via their modified ends.

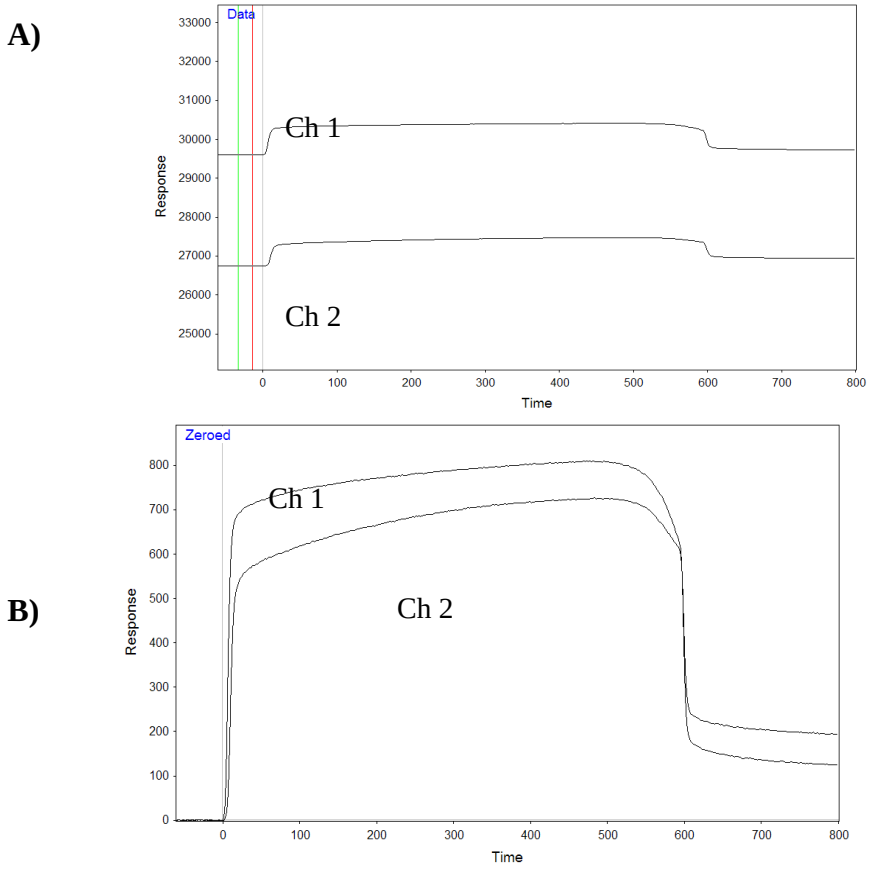

Figure 5.2 The immobilization of NAv-Maleimide modified ssDNA on the sensor surface A) before normalization of the responses at a zero state, B) after normalization.

5.1.3 Ligand (DNA) - Analyte (CRY-DASH and PHR) Interaction

The kinetic analysis of the ssDNA and CRY-DASH interaction is based on the calculation of response versus concentration of the analyte (CRY-DASH and PHR). For this purpose, the binding of the analyte at different concentrations was monitored by the SPR instrument (Figure 5.3). Figure 5.3A shows the immediate increase in binding during association phase. As the association phase reached the equilibrium, the binding of the

protein slightly decrease as shown with a small drop in response. The binding to UV-irradiated dsDNA started off very slowly as shown in Figure 5.3B. The increase in binding for UV-irradiated dsDNA was caused by the accumulation of the protein on sensor surface due to non-specific binding of CRY-DASH to UV-irradiated dsDNA. CRY-DASH was passed a second time to verify the non-specific binding on the accumulated protein. The binding of the protein was increased in the subsequent pass due to the non-specific binding to the protein that had been also bound non-specifically on dsDNA.

A)

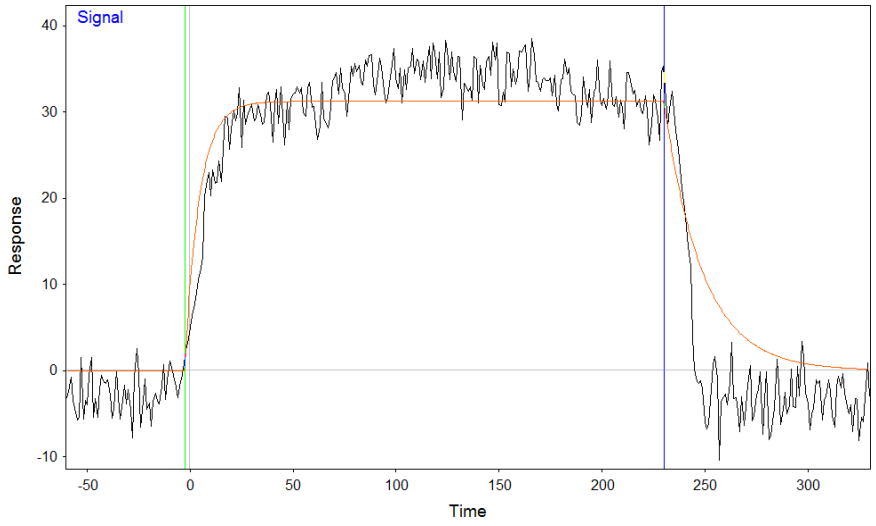

B)

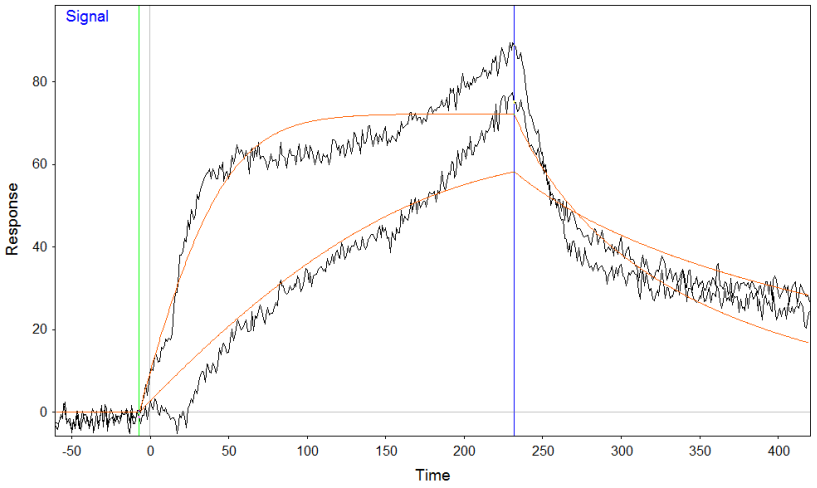

Figure 5.3 A) The response over time data for the CRY-DASH binding to UV-irradiated ssDNA. B) The response over time data for the CRY-DASH binding to UV-irradiated dsDNA.

The response obtained from PHR binding to UV-irradiated ssDNA and dsDNA was also measured (Figure 5.4). PHR bound more specifically to dsDNA than ssDNA, and it dissociated more readily and easily without accumulating on the surface. This was also proved in the kinetic constant calculations given in the next section. The number of the protein injections was increased for ssDNA case compared to the binding to dsDNA, to achieve the same total response for the protein binding on the surface, thus allowing the standardization of the amount of accumulation on the surface for both cases. The decreasing maximum response with the further PHR injections proves that the number of CPD sites to be bound decreases as PHR passes over UV-irradiated DNA

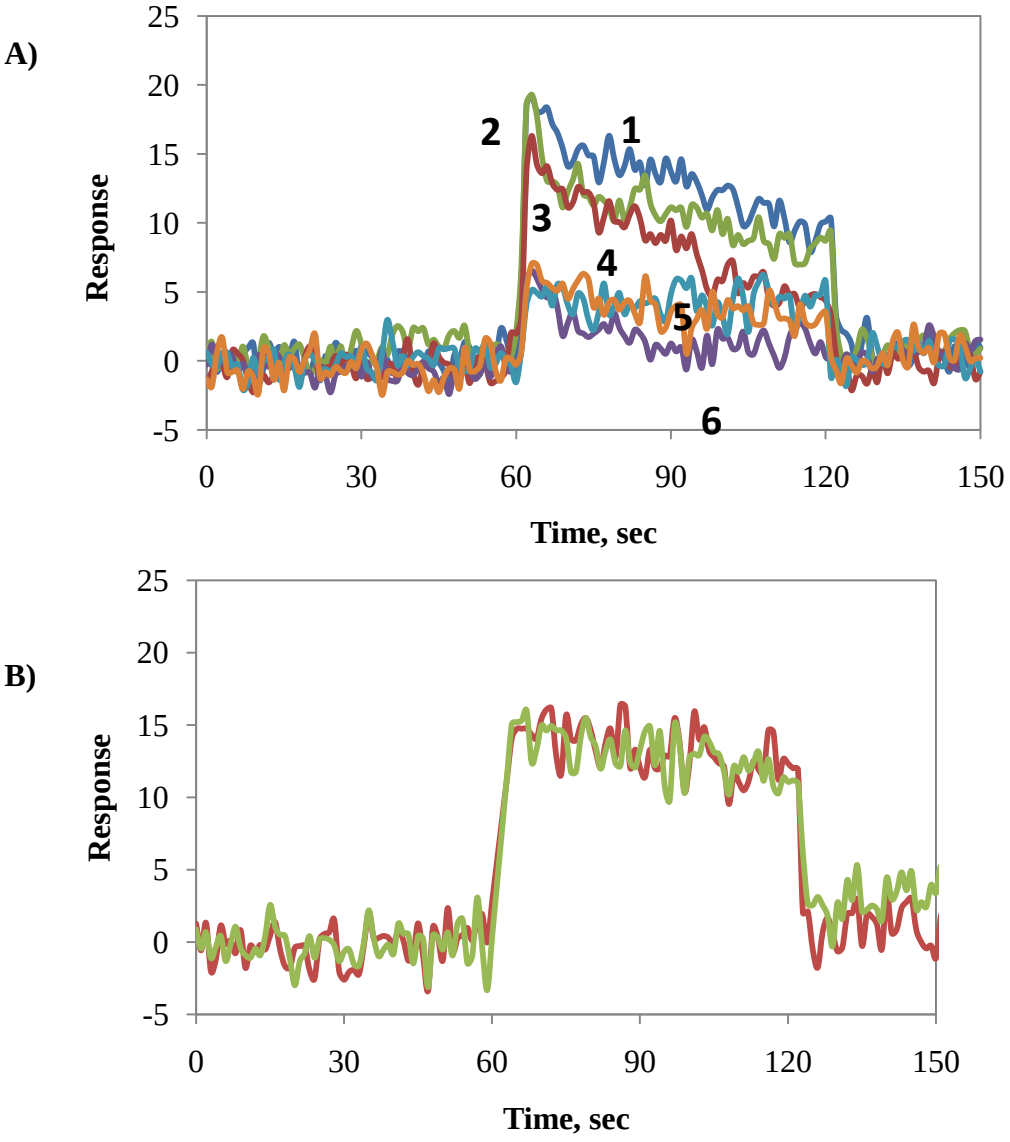

Figure 5.4 A) The response over time data for the PHR binding to UV-irradiated ssDNA. B) The response over time data for the PHR binding to UV-irradiated dsDNA.

In order to characterize the non-specific interaction of CRY-DASH with single or double strand DNA, un-irradiated ssDNA ana dsDNA was immobilized on sensor surface and its binding response was measured (Figure 5.5).

A)

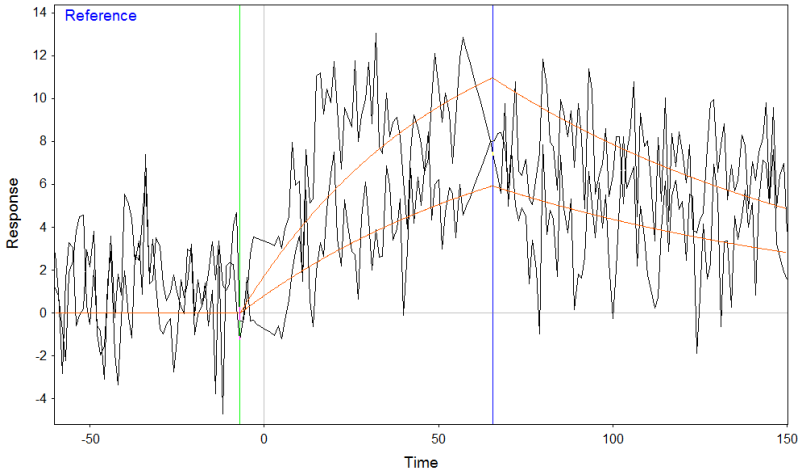

B)

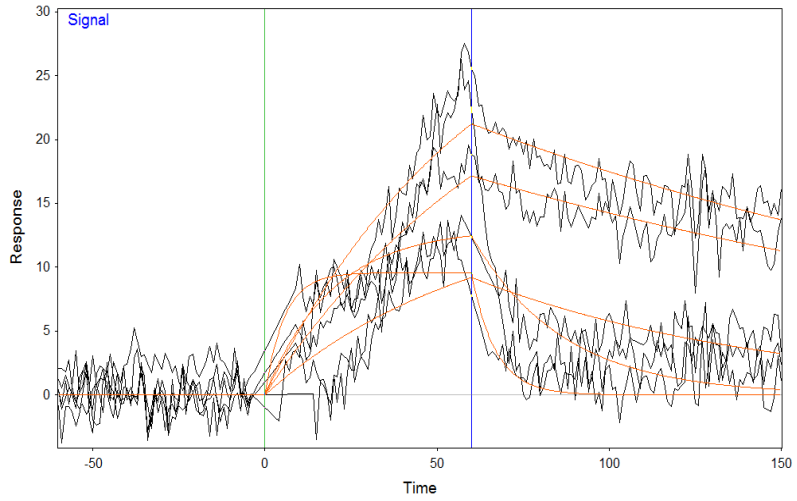

Figure 5.5 A) The response over time data for the CRY-DASH binding to un-irradiated ssDNA. B) The response over time data for the CRY-DASH binding to un-irradiated dsDNA.

PHR protein showed a significant amount of non-specific binding, which was also proven with the kinetic results in the section 5.1.4, and is shown in the Figure 5.6. The response for un-irradiated ssDNA and dsDNA started off rather slowly and reached its maximum at the end of injection, which is the beginning of the dissociation phase. This also indicates that the protein bound during the association phase continued to accumulate on the surface. Such an accumulation is related to non-specific binding of the protein, which was observed for non-specific binding of CRY-DASH on UV-irradiated dsDNA.

A)

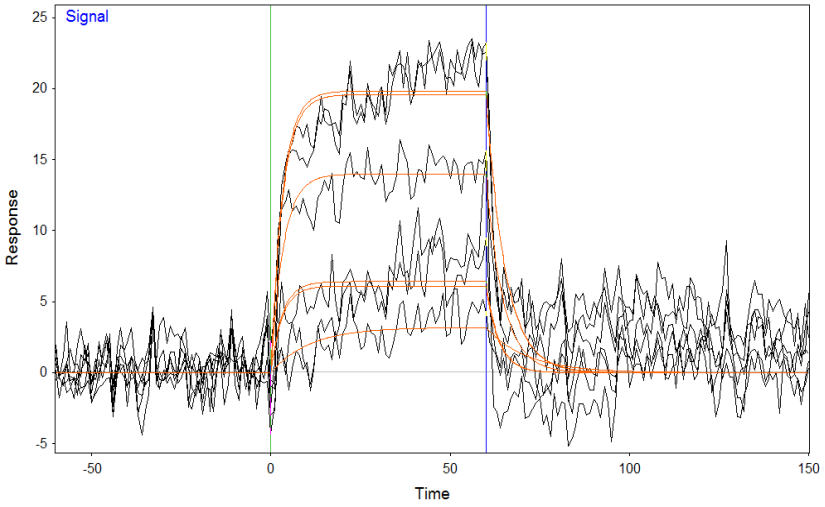

B)

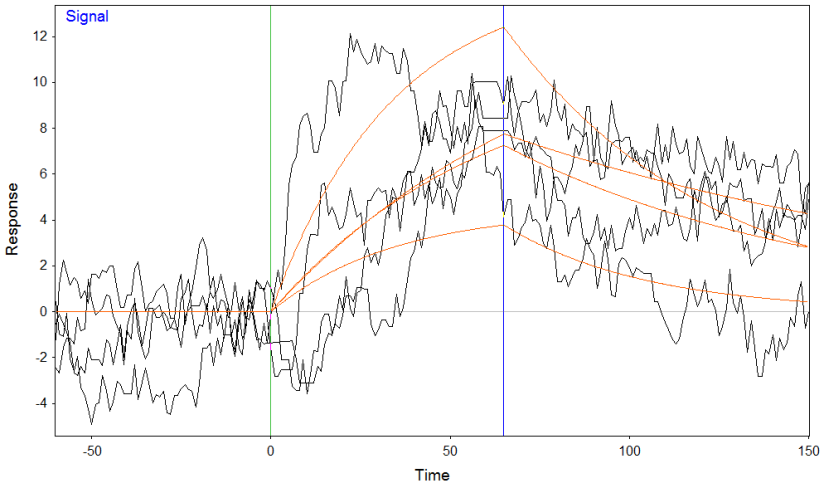

Figure 5.6 A) The response over time data for the PHR binding to un-irradiated ssDNA. B) The response over time data for the PHR binding to un-irradiated dsDNA.

5.1.4 Kinetic Results

The equilibrium constant (K_D) determination via kinetic calculations of Qdat provided the information about both the VcCRY I and PHR. Binding constant, K_D for PHR on un-irradiated dsDNA and ssDNA were estimated as 8.5 µM and 15.0 µM, respectively. On the other hand, binding constant K_D for PHR to CPD sites on double stranded DNA was 4.9 nM, while K_D was about equal to 50.9 nM for binding of PHR to single stranded DNA.

The K_D of CRY-DASH to un-irradiated dsDNA and ssDNA were calculated to be 16.9 µM and 620.9 nM respectively.

The kinetic results of binding of CRY-DASH to irradiated ssDNA gave a K_D value of 15.0 nM. The non-specific binding of CRY-DASH to UV-irradiated dsDNA was found to be 22.9 µM. Since K_D is the ratio of k_d over k_a as given in equation (3.1), lower K_D values indicates a more dominant association constant compared to the dissociation constant.

Consequently, this means higher affinity for the binding of the components of the system. Conversely, higher K_D value is the indicative of much lower affinity between the analyte and ligand.

Table 5.1 Equilibrium Dissociation Constant Values Obtained from Qdat Analysis Program for PHR and CRY-DASH

	KD	**Res SD (RU)**	**Rmax (RU)**
PHR + Undamaged dsDNA	8.5 uM	2.52	35
PHR + Undamaged ssDNA	15.0 uM	1.37	50
PHR + Damaged dsDNA	4.9 nM	3.48	50
PHR + Damaged ssDNA	50.9 nM	1.75	35
CRY + Undamaged dsDNA	16.9 uM	2.39	50
CRY + Undamaged ssDNA	60.9 nM	2.13	35
CRY+ Damaged dsDNA	22.9 uM	6.16	100
CRY + Damaged ssDNA	15.0 nM	4.94	50

A more detailed investigation of the kinetic results was given in Section 6.3.

Chapter 6

6. DISCUSSION

More detailed investigation of the SPR results will be provided in this section.

6.1 SPR Data Processing

The kinetic analysis or the equilibrium calculations were made by the Qdat Data Analysis program. The program uses the interface that stores and visualizes the data monitored during SPR experiments, and also offers the possibility to specify the experiment details as additional inputs (Figure 6.1).

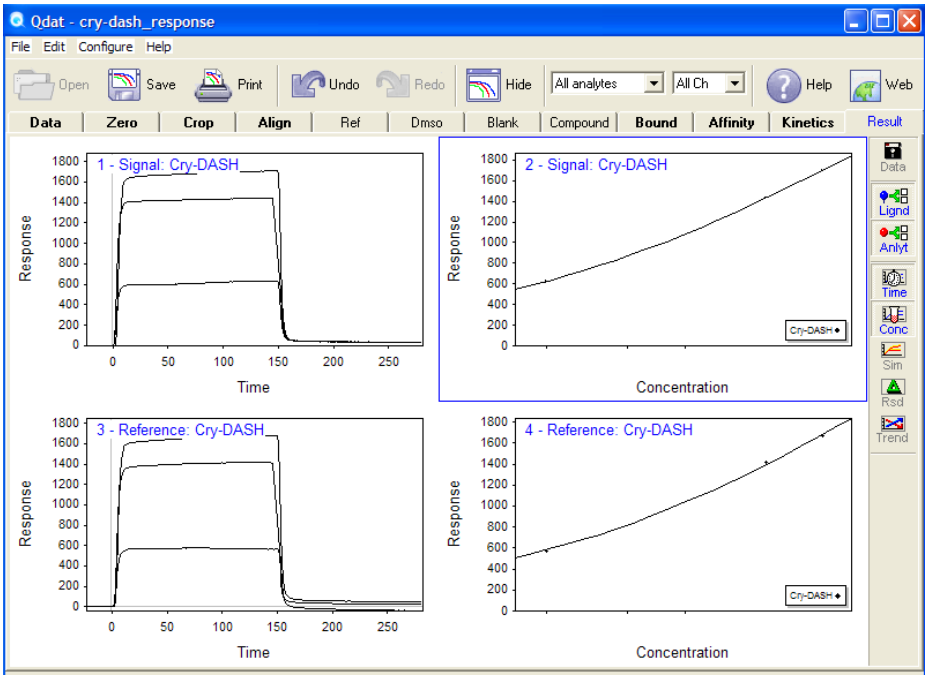

Figure 6.1 The user interface for Qdat Data Analysis program

For all SPR results, it is important to filter the response data that is otherwise spoiled because of the air spikes in injection lines. These response dips were eliminated using the data cut function of Sensiq Discovery program used for real-time binding observation.

6.2 SPR Equilibrium Analysis

The choice of the analysis method whether to be kinetic or equilibrium was determined according to the interaction speed [63]. For CRY-DASH – ssDNA interaction, kinetic analysis seems to be more suitable since the association and dissociation of the protein to DNA is fast. Even though it is hard to get a sensitive recording on the repair mechanism, the repair process can be observed over the equilibrium plateau. A slower rate of binding enables the use of kinetic analysis but both results should have similar K_D values in order to be defined as reliable. Ideally, analyte concentration should be varied about three orders of magnitude, from $0.01*K_D$ to $100*K_D$ in order to obtain accurate binding constant of interaction. Therefore, in this study CRY-DASH concentration was chosen to vary from 1 nM to 100 nM. PHR and CRY-DASH constants were generally determined by their relative affinity to the DNA strand of choice because the kinetic calculations are very much dependent on concentration range. The typical equilibrium constant for interaction between CRY-DASH and single stranded DNA is known to be around $K_D \approx 10^{-7}$, and 10-fold higher than K_D of PHR [64, 65].

In addition, for affinity measurement experiments, the level of active immobilized ligand was assumed to remain constant. The validity of this assumption was investigated further by comparing the analyte response for reference channel at the beginning, and at the end of the experiment. Figure 6.2 shows the analyte response at the reference channel, and confirms that after the dissociation of CRY-DASH, there was no DNA removed from the surface because the response curve returned to its original value before the association of the protein.

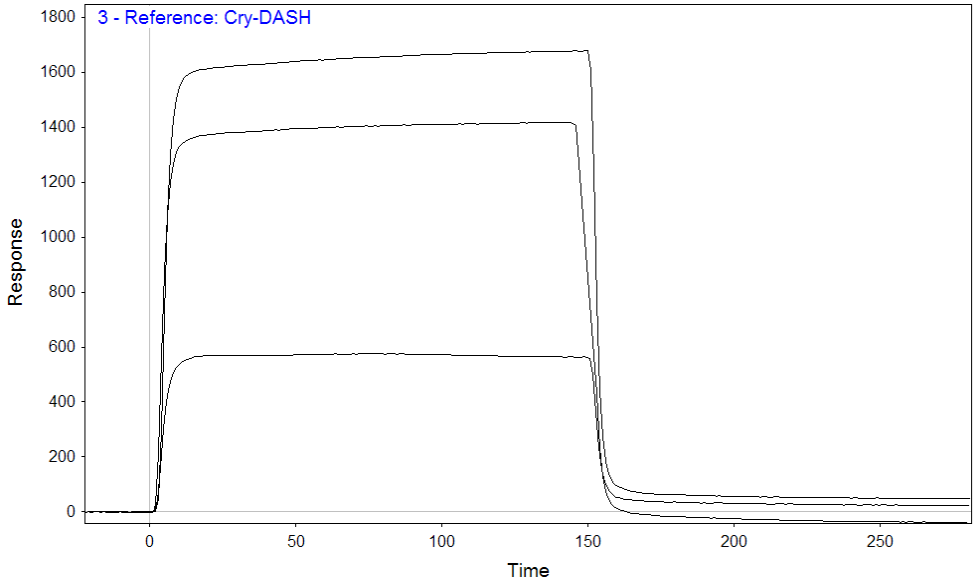

Figure 6.2 SPR response over time curves for undamaged ssDNA immobilized sensor surfaces.

As observed in figure 6.3, if one of the assay cycles shows significant decrease between the beginning and end of the injection, then it is possible that some of the immobilized DNA molecules are removed from the surface. The removal of DNA requires the breakage of the biotin-avidin linkage, which also requires extreme conditions to break. Under this condition it is possible that some of the ssDNA had bound non-specifically to the surface (not through biotin-avidin interaction). In this case, the assay should be repeated again after cleaning the surface (0.1% SDS, 0.1 M NaOH). Surface treatment with SDS and NaOH on the other hand doesn't remove the ssDNA that is specifically bound via biotin-avidin linkage. So, it should also be considered that if the same sensor chip is used next time, the surface will already be covered with ssDNA molecules.

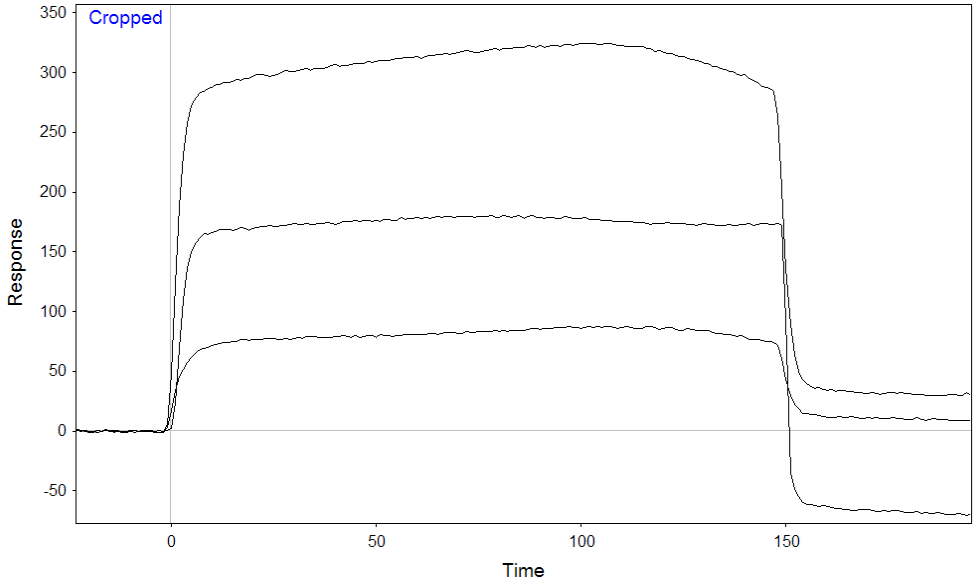

Figure 6.3 Response over time data for different concentrations of CRY-DASH showing the removal of DNA from the surface.

If the DNA immobilization on sensor surface was proved to be stable as required, then the assay would continue with the injection of the analyte, which in this case is CRY-DASH. The analyte was injected at different concentrations for data processing to be more reliable since the global curve fitting of the results by Qdat data analysis program would give more reliable simulations of the association, equilibrium and dissociation phases.

As was described in earlier section, if the binding rate of the analyte to the immobilized ligand is fast enough, it is more appropriate to perform equilibrium analysis on the system, and to use relatively higher concentrations. This can be tested by comparing low concentration data with the higher concentrations. For CRY-DASH and ssDNA interaction, it is possible to achieve kinetic controlled interaction below 2.5 nM. But at the same time it was difficult to monitor the binding of CRY-DASH below this level, since the

quality of data decreases at this level of concentration due to the limitation of the instrument. A simple CRY-DASH response for concentration of 2.5 nM is shown in Figure 6.4.

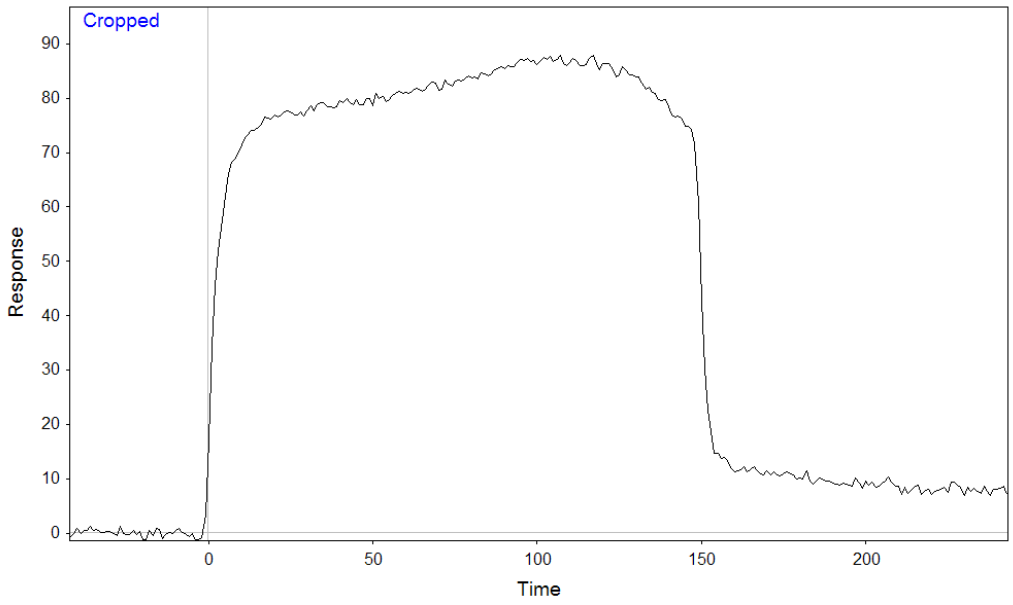

Figure 6.4 Response over time data for CRY-DASH concentration of 2.5 nM - the surface was immobilized with UV-irradiated ssDNA.

As Figure 6.4 shows, the variations in response become more pronounced as the maximum response reached, and remains below 100 response units. The minimum RU limit for reliable data analysis varies near 5-10 RU. Below that point, it becomes difficult to differentiate the real response from baseline drifts and temperature variations because of the lack of a temperature control system on our SPR instrument.

A more appropriate example of comparison of low and high concentrations of CRY-DASH is shown in figure 6.5 given below. This data also is a more clear representation of a qualitative analysis on CRY-DASH and ssDNA interaction.

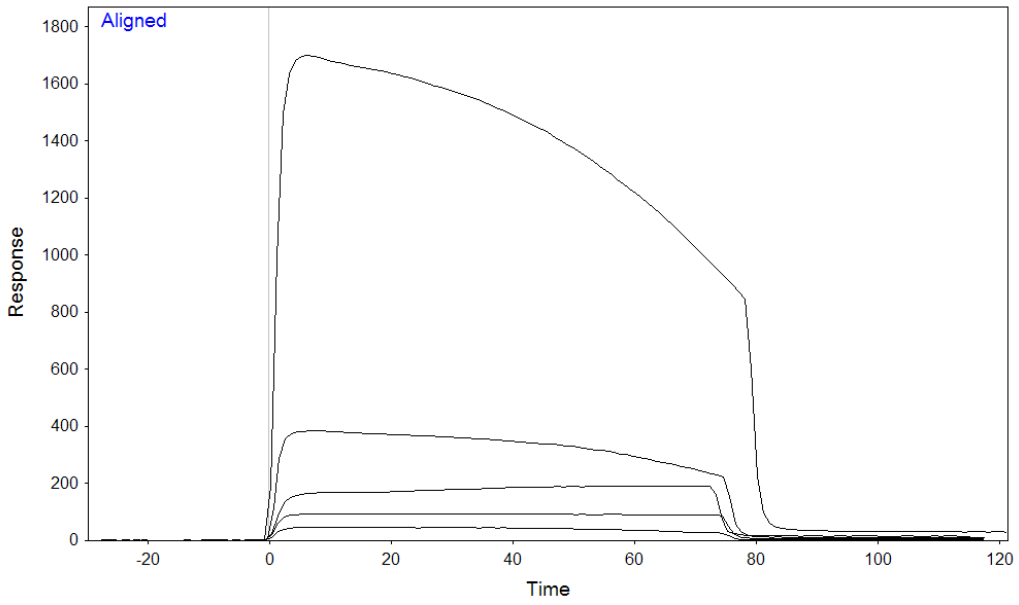

Figure 6.5 Response over time data for CRY-DASH concentrations of 1.25, 2.5, 5, 10 and 20 nM - the surface was immobilized with UV-irradiated ssDNA.

While the kinetic and equilibrium analysis quantitatively investigate the association, dissociation and/or equilibrium phases provide the rate constants about the interaction of interest, and qualitative analysis makes it possible to observe and comment on the general behavior of the analyte against the ligand. The figure suggests that at higher concentrations, the CRY-DASH response starts to dissipate from the surface quickly after association phase even though the protein concentration of the sample buffer doesn't change. It is

highly possible that the higher amounts of the protein dissociate as a result of mass transport limitations, thus was able to cover most of the CPD sites on ssDNA quickly and repair those sites. The common repair mechanism suggests that the repair proteins depart from the DNA strand immediately after the repair [64, 66] which takes place in tens to hundreds picoseconds [67, 68]. In SPR measurements, this phenomenon can be significantly observed only at the concentrations above 5 nM due to the limitations of the instrument.

6.3 Rate constants

K_D for the binding of PHR on un-irradiated dsDNA was estimated as 8.5 μM whereas K_D for the binding of PHR on un-irradiated ssDNA was estimated as 15.0 μM. The micro molar level of K_D is considered as a sign of non-specific binding due to its much higher value. The equilibrium constants of PHR for binding to UV-irradiated DNA were found to be much less than un-irradiated DNA with the following results. The higher affinity of PHR to CPD sites on double stranded DNA was observed with a K_D of 4.9 nM. This was also similar with PHR binding to single stranded DNA despite with a lesser affinity than that of PHR to dsDNA (K_D ~ 50.9 nM). The SPR data also showed satisfactory results that prove the non-specific binding of CRY-DASH to un-irradiated DNA. The equilibrium constant of the protein to un-irradiated dsDNA and ssDNA were calculated to be 16.9 μM and 620.9 nM respectively. The non-specific binding of CRY-DASH to un-irradiated ssDNA still shows much higher affinity than the non-specific binding to dsDNA with a K_D of 620.9 nM. It is thought to be related with the CRY-DASH binding cavity, which allows catching the CPD site over a single DNA strand inside easier compared to the binding that would take place with double strand DNA. However, CRY-DASH always binds to dsDNA non-specifically even if it is irradiated, which was observed with K_D values of 22.9 μM and 16.9 μM for UV-irradiated dsDNA, and for un-irradiated dsDNA, respectively. The sensitivity on the kinetic data can be increased by using DNA

strands containing higher number of thymine dimers, which increases the chance of CPD formation during UV-irradiation. Higher number of CPD sites should allow more proteins to bind to DNA strands.

A significant increase in binding affinity of CRY-DASH to irradiated ssDNA compared to irradiated dsDNA was observed as also was measured with higher PHR affinity to dsDNA compared to that affinity with ssDNA. The results gave a K_D value of 15.0 nM for irradiated dsDNA with CRY-DASH.

The literature on CRY-DASH kinetic constants are in much less in number compared to PHR and vary in broad range [64, 65, 67]. This was due to the varying methods used to measure the kinetic parameters and especially due to lack of studies done on CRY-DASH kinetics. However, our data were still comparable to the literature equilibrium dissociation rates in the same range ($\sim 10^{-8}$ for PHR and suggesting an approximate value of $\sim 10^{-7}$ for CRY-DASH) [64, 65]. According to the values obtained in this study and supported by previous studies[5], significant difference found between binding of CRY-DASH to ssDNA and to dsDNA. In this study, the binding kinetic constant values between CRY-DASH and DNA has been found for the first time in literature.. Also, PHR binds specifically to UV-irradiated dsDNA, unlike CRY-DASH as was calculated from the binding profiles.

Interestingly, the response curves for non-specific binding of both CRY-DASH and PHR binding to dsDNA were proved to be similar. This can be an indication of a common protein-DNA interaction for CRY-DASH and PHR to DNA, if they are bound non-specifically (Figure 5.5 and 5.6).

Another interesting observation with the SPR results is that longer injection times allow the user to observe small changes in binding of the analyte during the association

phase. These small changes indicate different means of interactions and possible reactions between the analyte and the ligand other than the affinity between analyte and ligand. The duration of injection for CRY-DASH and PHR to UV-irradiated ssDNA was kept longer than normal association phase used in the other binding experiments intentionally. It was observed that a small decrease in binding during association phase after some time interval. This has been observed for the first time in the literature with SPR, and is possibly due to the increased number of repaired CPD sites which were no longer prone to specific binding of the repair enzymes. The decrease in response unit during injection phase is also consistent with the existing biological DNA repair mechanism which suggests dissociation of repair protein from DNA very fast after repair process even during injection phase of the repair protein.

Here, it can be proposed that CRY-DASH may have some RNA specific repair mechanism as PHR has on dsDNA since the single stranded structure of RNA. This can be also related to the need of some repair measures for the errors during transcription, that are inherited to mRNA. A further investigation is necessary for CRY-DASH and RNA relationship.

Finally, for further investigation of ssDNA repair by CRY-DASH, it is possible to use UV-irradiated ssDNA samples that are treated with CRY-DASH prior to SPR assay. This can support the data presented in this work and may suggest a specific binding between UV-irradiated ssDNA and CRY-DASH. Pre-treatment with CRY-DASH should repair the CPD sites on ssDNA, and a subsequent SPR assay should show non-specific binding of CRY-DASH to the ssDNA which already get its CPD sites repaired to the original thymine dimers during pre-treatment.

The quality of the data analyzed was then measured by the residual standard deviation over maximum response ratio (Res_{SD} / RU_{max}) in Table 6.1:

Table 6.1. Residual standard deviation over maximum response ratio results for the curve fittings

Repair Protein + DNA Sample	**Res_{SD} / RU_{max}**	**Result**
PHR + Undamaged dsDNA	2.52/35	0.07
PHR + Undamaged ssDNA	1.37/50	0.03
PHR + Damaged dsDNA	3.48/50	0.07
PHR + Damaged ssDNA	1.75/35	0.05
CRY + Undamaged dsDNA	2.40/50	0.05
CRY + Undamaged ssDNA	2.13/35	0.06
CRY + Damaged dsDNA	6.16/100	0.06
CRY + Damaged ssDNA	4.94/50	0.10

The values below 0.1 are desirable for successful results. For all the experiments performed, values lower than 0.1 were obtained. It is limited to reach better results due to the inadequate global curve fitting of the analysis program. The viability of curve fitting relies on the permanence of the ligand and the analyte for each cycle of the assay. Mass transport limitations were non-existent for our experiment due to the precautions taken (high concentration and flow rate of the analyte, low amount of surface coverage with our ligand). This was proved by the MTL (Mass Transport Limitation) function of the Qdat Data Analysis program (Figure 6.6).

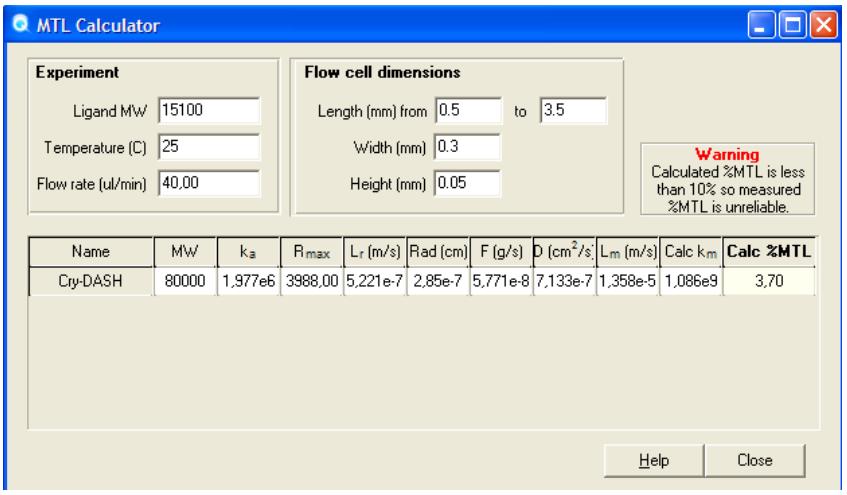

Figure 6.6 Mass transport calculator result for the equilibrium analysis done.

As Figure 6.6 shows, the effect of mass transport limitation on equilibrium analysis was less than %10, which ensures that the standard binding model was sufficient to calculate kinetic and equilibrium constants. Percent mass transport limitation effect on the binding model depends on the flow cell dimension, molecular weight of the ligand, and the flow rate of the buffer used.

Chapter 7

7. CONCLUSION

In this thesis, the affinity of a photolyase/cryptochrome family protein, CRY-DASH, to the UV-irradiated single stranded DNA was investigated. The affinity and binding kinetics were investigated by Surface Plasmon Resonance of the DNA-protein binding real-time, and data analysis according to the simple 1:1 DNA-CRY binding model.

SPR results confirmed higher affinity of CRY-DASH to CPD (cyclobutane prymidine dimer) containing single stranded DNA by giving lower K_D value (K_D of 15 nM for UV-irradiated ssDNA). A significant difference was found between specific and non-specific binding of CRY-DASH to ssDNA and dsDNA, as was observed in previous studies [20, 22, 64]. It is important to note that the exact literature values of equilibrium constants specific for VcCRY I, were non-existent up to date. The comparison of PHR affinity to CPD containing ssDNA from the data found in literature suggests that our results are consistent with earlier findings (PHR gives a K_D of 4.9 nM). This suggests SPR as a reliable assay to characterize binding and repair of DNA by both PHR and CRY-DASH.

The specifications for the experimental setup could be improved by complete temperature control and a faraday cage to prevent outer electromagnetic effects that cause noise in SPR signals. Other experimental methods can also be used to measure kinetic constants to determine a suitable binding model and to compare them with the SPR results. The typical SPR results should also be analyzed with analytical ultracentrifugation[69] and isothermal titration calorimetry [70]. Finally, this study is original as it suggests for the first time in the literature that it is possible to investigate the real time DNA repair via SPR, and that the level of interaction of DNA with repair proteins can be quantified.

BIBLIOGRAPHY

1. Weber, S., *Light-driven enzymatic catalysis of DNA repair: a review of recent biophysical studies on photolyase.* Biochim Biophys Acta, 2005. **1707**(1): p. 1-23.
2. Guo, H., et al., *The Arabidopsis blue light receptor cryptochrome 2 is a nuclear protein regulated by a blue light-dependent post-transcriptional mechanism.* Plant J, 1999. **19**(3): p. 279-87.
3. Lin, C., *Plant blue-light receptors.* Trends Plant Sci, 2000. **5**(8): p. 337-42.
4. King, D.P. and J.S. Takahashi, *Molecular genetics of circadian rhythms in mammals.* Annu Rev Neurosci, 2000. **23**: p. 713-42.
5. Selby, C.P. and A. Sancar, *A cryptochrome/photolyase class of enzymes with single-stranded DNA-specific photolyase activity.* Proc Natl Acad Sci U S A, 2006. **103**(47): p. 17696-700.
6. Roulston, A., R.C. Marcellus, and P.E. Branton, *Viruses and apoptosis.* Annu Rev Microbiol, 1999. **53**: p. 577-628.
7. Browner, W.S., et al., *The genetics of human longevity.* Am J Med, 2004. **117**(11): p. 851-60.
8. Cleaver, J.E. and E. Crowley, *UV damage, DNA repair and skin carcinogenesis.* Front Biosci, 2002. **7**: p. d1024-43.
9. Donahue, B.A., et al., *Transcript cleavage by RNA polymerase II arrested by a cyclobutane pyrimidine dimer in the DNA template.* Proc Natl Acad Sci U S A, 1994. **91**(18): p. 8502-6.
10. Hanawalt, P.C., *Transcription-coupled repair and human disease.* Science, 1994. **266**(5193): p. 1957-8.
11. Otoshi, E., et al., *Respective roles of cyclobutane pyrimidine dimers, (6-4)photoproducts, and minor photoproducts in ultraviolet mutagenesis of repair-deficient xeroderma pigmentosum A cells.* Cancer Res, 2000. **60**(6): p. 1729-35.
12. Gilchrest, B.A., et al., *The pathogenesis of melanoma induced by ultraviolet radiation.* N Engl J Med, 1999. **340**(17): p. 1341-8.
13. Adimoolam, S. and J.M. Ford, *p53 and regulation of DNA damage recognition during nucleotide excision repair.* DNA Repair (Amst), 2003. **2**(9): p. 947-54.
14. You, Y.H., P.E. Szabo, and G.P. Pfeifer, *Cyclobutane pyrimidine dimers form preferentially at the major p53 mutational hotspot in UVB-induced mouse skin tumors.* Carcinogenesis, 2000. **21**(11): p. 2113-7.
15. Essen, L.O., *Photolyases and cryptochromes: common mechanisms of DNA repair and light-driven signaling?* Curr Opin Struct Biol, 2006. **16**(1): p. 51-9.
16. Sancar, A., *Structure and function of DNA photolyase and cryptochrome blue-light photoreceptors.* Chemical Reviews, 2003. **103**(6): p. 2203-37.
17. Muller, M. and T. Carell, *Structural biology of DNA photolyases and cryptochromes.* Current Opinion in Structural Biology, 2009. **19**(3): p. 277-285.
18. Li, Q.H. and H.Q. Yang, *Cryptochrome signaling in plants.* Photochem Photobiol, 2007. **83**(1): p. 94-101.
19. van der Horst, G.T., et al., *Mammalian Cry1 and Cry2 are essential for maintenance of circadian rhythms.* Nature, 1999. **398**(6728): p. 627-30.

20. Daiyasu, H., et al., *Identification of cryptochrome DASH from vertebrates.* Genes Cells, 2004. **9**(5): p. 479-95.
21. Kleine, T., P. Lockhart, and A. Batschauer, *An Arabidopsis protein closely related to Synechocystis cryptochrome is targeted to organelles.* Plant J, 2003. **35**(1): p. 93-103.
22. Brudler, R., et al., *Identification of a new cryptochrome class. Structure, function, and evolution.* Mol Cell, 2003. **11**(1): p. 59-67.
23. Huang, Y., et al., *Crystal structure of cryptochrome 3 from Arabidopsis thaliana and its implications for photolyase activity.* Proc Natl Acad Sci U S A, 2006. **103**(47): p. 17701-6.
24. Komori, H., et al., *Crystal structure of thermostable DNA photolyase: pyrimidine-dimer recognition mechanism.* Proc Natl Acad Sci U S A, 2001. **98**(24): p. 13560-5.
25. Park, H.W., et al., *Crystal structure of DNA photolyase from Escherichia coli.* Science, 1995. **268**(5219): p. 1866-72.
26. Brautigam, C.A., et al., *Structure of the photolyase-like domain of cryptochrome 1 from Arabidopsis thaliana.* Proc Natl Acad Sci U S A, 2004. **101**(33): p. 12142-7.
27. Mees, A., et al., *Crystal structure of a photolyase bound to a CPD-like DNA lesion after in situ repair.* Science, 2004. **306**(5702): p. 1789-93.
28. Heidelberg, J.F., et al., *DNA sequence of both chromosomes of the cholera pathogen Vibrio cholerae.* Nature, 2000. **406**(6795): p. 477-83.
29. Cunningham, B.C. and J.A. Wells, *Comparison of a structural and a functional epitope.* J Mol Biol, 1993. **234**(3): p. 554-63.
30. Johanson, K., et al., *Binding interactions of human interleukin 5 with its receptor alpha subunit. Large scale production, structural, and functional studies of Drosophila-expressed recombinant proteins.* J Biol Chem, 1995. **270**(16): p. 9459-71.
31. Holliger, P., T. Prospero, and G. Winter, *"Diabodies": small bivalent and bispecific antibody fragments.* Proc Natl Acad Sci U S A, 1993. **90**(14): p. 6444-8.
32. Kelley, R.F. and M.P. O'Connell, *Thermodynamic analysis of an antibody functional epitope.* Biochemistry, 1993. **32**(27): p. 6828-35.
33. Malmborg, A.C. and C.A. Borrebaeck, *BIAcore as a tool in antibody engineering.* J Immunol Methods, 1995. **183**(1): p. 7-13.
34. Glaser, R.W. and G. Hausdorf, *Binding kinetics of an antibody against HIV p24 core protein measured with real-time biomolecular interaction analysis suggest a slow conformational change in antigen p24.* J Immunol Methods, 1996. **189**(1): p. 1-14.
35. Pellequer, J.L. and M.H. Van Regenmortel, *Measurement of kinetic binding constants of viral antibodies using a new biosensor technology.* J Immunol Methods, 1993. **166**(1): p. 133-43.
36. Schasfoort, R.B.M. and A.J. Tudos, *Handbook of surface plasmon resonance*. 2008, Cambridge, UK: RSC Pub. xxi, 403 p.
37. van der Merwe, P.A. and A.N. Barclay, *Analysis of cell-adhesion molecule interactions using surface plasmon resonance.* Curr Opin Immunol, 1996. **8**(2): p. 257-61.
38. Buckle, M., et al., *Real time measurements of elongation by a reverse transcriptase using surface plasmon resonance.* Proc Natl Acad Sci U S A, 1996. **93**(2): p. 889-94.

39. Fisher, R.J. and M. Fivash, *Surface plasmon resonance based methods for measuring the kinetics and binding affinities of biomolecular interactions.* Curr Opin Biotechnol, 1994. **5**(4): p. 389-95.
40. Di Primo, C. and I. Lebars, *Determination of refractive index increment ratios for protein-nucleic acid complexes by surface plasmon resonance.* Analytical Biochemistry, 2007. **368**(2): p. 148-55.
41. Alam, S.M., et al., *T-cell-receptor affinity and thymocyte positive selection.* Nature, 1996. **381**(6583): p. 616-20.
42. Corr, M., et al., *T cell receptor-MHC class I peptide interactions: affinity, kinetics, and specificity.* Science, 1994. **265**(5174): p. 946-9.
43. MacKenzie, C.R., et al., *Analysis by surface plasmon resonance of the influence of valence on the ligand binding affinity and kinetics of an anti-carbohydrate antibody.* J Biol Chem, 1996. **271**(3): p. 1527-33.
44. Gotoh, M., et al., *A new approach to determine the effect of mismatches on kinetic parameters in DNA hybridization using an optical biosensor.* DNA Res, 1995. **2**(6): p. 285-93.
45. Johnsson, B., et al., *Comparison of methods for immobilization to carboxymethyl dextran sensor surfaces by analysis of the specific activity of monoclonal antibodies.* J Mol Recognit, 1995. **8**(1-2): p. 125-31.
46. Stein, T. and G. Gerisch, *Oriented binding of a lipid-anchored cell adhesion protein onto a biosensor surface using hydrophobic immobilization and photoactive crosslinking.* Analytical Biochemistry, 1996. **237**(2): p. 252-9.
47. Bernard, A. and H.R. Bosshard, *Real-time monitoring of antigen-antibody recognition on a metal oxide surface by an optical grating coupler sensor.* Eur J Biochem, 1995. **230**(2): p. 416-23.
48. Jost, J.P., O. Munch, and T. Andersson, *Study of protein-DNA interactions by surface plasmon resonance (real time kinetics).* Nucleic Acids Research, 1991. **19**(10): p. 2788.
49. Bondeson, K., et al., *Lactose repressor-operator DNA interactions: kinetic analysis by a surface plasmon resonance biosensor.* Analytical Biochemistry, 1993. **214**(1): p. 245-51.
50. Karlsson, R., A. Michaelsson, and L. Mattsson, *Kinetic analysis of monoclonal antibody-antigen interactions with a new biosensor based analytical system.* J Immunol Methods, 1991. **145**(1-2): p. 229-40.
51. Ladbury, J.E., et al., *Measurement of the binding of tyrosyl phosphopeptides to SH2 domains: a reappraisal.* Proc Natl Acad Sci U S A, 1995. **92**(8): p. 3199-203.
52. Matsui, K., et al., *Kinetics of T-cell receptor binding to peptide/I-Ek complexes: correlation of the dissociation rate with T-cell responsiveness.* Proc Natl Acad Sci U S A, 1994. **91**(26): p. 12862-6.
53. O'Shannessy, D.J., *Determination of kinetic rate and equilibrium binding constants for macromolecular interactions: a critique of the surface plasmon resonance literature.* Curr Opin Biotechnol, 1994. **5**(1): p. 65-71.
54. Karlsson, R. and R. Stahlberg, *Surface plasmon resonance detection and multispot sensing for direct monitoring of interactions involving low-molecular-weight analytes and for determination of low affinities.* Analytical Biochemistry, 1995. **228**(2): p. 274-80.

55. Northrup, S.H. and H.P. Erickson, *Kinetics of protein-protein association explained by Brownian dynamics computer simulation.* Proc Natl Acad Sci U S A, 1992. **89**(8): p. 3338-42.
56. Felder, S., et al., *SH2 domains exhibit high-affinity binding to tyrosine-phosphorylated peptides yet also exhibit rapid dissociation and exchange.* Mol Cell Biol, 1993. **13**(3): p. 1449-55.
57. van der Merwe, P.A., et al., *Affinity and kinetic analysis of the interaction of the cell adhesion molecules rat CD2 and CD48.* Embo Journal, 1993. **12**(13): p. 4945-54.
58. Silhavy, T.J., et al., *On the significance of the retention of ligand by protein.* Proc Natl Acad Sci U S A, 1975. **72**(6): p. 2120-4.
59. Glaser, R.W., *Antigen-antibody binding and mass transport by convection and diffusion to a surface: a two-dimensional computer model of binding and dissociation kinetics.* Analytical Biochemistry, 1993. **213**(1): p. 152-61.
60. Schuck, P. and A.P. Minton, *Analysis of mass transport-limited binding kinetics in evanescent wave biosensors.* Analytical Biochemistry, 1996. **240**(2): p. 262-72.
61. Worthington, E.N., et al., *Purification and characterization of three members of the photolyase/cryptochrome family blue-light photoreceptors from Vibrio cholerae.* Journal of Biological Chemistry, 2003. **278**(40): p. 39143-39154.
62. Cannon, M.J., et al., *Comparative analyses of a small molecule/enzyme interaction by multiple users of Biacore technology.* Analytical Biochemistry, 2004. **330**(1): p. 98-113.
63. Myszka, D.G., et al., *Kinetic analysis of a protein antigen-antibody interaction limited by mass transport on an optical biosensor.* Biophys Chem, 1997. **64**(1-3): p. 127-37.
64. Sancar, G.B., et al., *Action mechanism of Escherichia coli DNA photolyase. III. Photolysis of the enzyme-substrate complex and the absolute action spectrum.* J Biol Chem, 1987. **262**(1): p. 492-8.
65. McLeod, N.R., et al., *Distinct recognition loop dynamics in cryptochrome-DASH and photolyase revealed by limited proteolysis.* Biochem Biophys Res Commun, 2009. **385**(3): p. 424-9.
66. Pokorny, R., et al., *Recognition and repair of UV lesions in loop structures of duplex DNA by DASH-type cryptochrome.* Proc Natl Acad Sci U S A, 2008. **105**(52): p. 21023-7.
67. Chang, C.W., et al., *Ultrafast solvation dynamics at binding and active sites of photolyases.* Proc Natl Acad Sci U S A, 2010. **107**(7): p. 2914-9.
68. Heelis, P.F., T. Okamura, and A. Sancar, *Excited-state properties of Escherichia coli DNA photolyase in the picosecond to millisecond time scale.* Biochemistry, 1990. **29**(24): p. 5694-8.
69. Hensley, P., *Defining the structure and stability of macromolecular assemblies in solution: the re-emergence of analytical ultracentrifugation as a practical tool.* Structure, 1996. **4**(4): p. 367-73.
70. Doyle, M.L., D.G. Myszka, and I.M. Chaiken, *Molecular interaction analysis in ligand design using mass transport, kinetic and thermodynamic methods.* J Mol Recognit, 1996. **9**(2): p. 65-74.

VITA

Enis Demir was born in İstanbul, Turkey, on December 20, 1985. He received her B.Sc. Degree in Chemical and Biological Engineering from Koç University, Istanbul, in 2008. From September 2008 to August 2010 he worked as teaching and research assistant at Koç University, Istanbul, Turkey. He has worked on “Characterization of Real Time DNA Repair via Surface Plasmon Resonance (SPR)” during his M.S. study.